Cretaceous-Paleocene evolution and crustal structure of the northern Vøring Margin (offshore Mid-Norway): results from integrated geological and geophysical study

D. Zastrozhnov[1,2*], L. Gernigon[3], I. Gogin[4], M.M. Abdelmalak[1], S.Planke[1,2], J.I. Faleide[1], S. Eide[5] and R.Myklebust[6]

[1]Centre for Earth Evolution and Dynamics (CEED), University of Oslo, Norway

[2]Volcanic Basin Petroleum Research (VBPR), Oslo Science Park, Oslo, Norway

[3]Geological Survey of Norway (NGU), Trondheim, Norway

[4]RPS Ichron, Northwich, Cheshire, UK

[5]First Geo AS, Skøyen, Norway

[6]TGS, Asker, Norway

*Corresponding author: Dmitry Zastrozhnov (zastrozhe@gmail.com)

Key Points:

- New multidisciplinary geological study of the northern Vøring Margin
- Early to mid-Cretaceous local phases of extensional reactivation in the mid-Norwegian margin
- Role of inherited crustal "buffers" in the development of sag basins

This article has been accepted for publication and undergone full peer review but has not been through the copyediting, typesetting, pagination and proofreading process which may lead to differences between this version and the Version of Record. Please cite this article as doi: 10.1002/2017TC004655

ABSTRACT

We present results of a multidisciplinary study of the northern segment of the Vøring volcanic rifted margin, offshore mid-Norway. This segment represents a transitional margin domain that is less investigated compared to the adjacent segments of the margin. In order to understand the geological evolution of the study area, we performed an integrated geophysical and geological interpretation of an extensive geophysical dataset. This dataset includes recently acquired and reprocessed 2D reflection seismic, published refraction data and potential field data, as well as new borehole data. 2D potential field modelling was performed to better assess the crustal architecture and evolution of the northern Vøring Margin. We then consider how crustal-scale structures and processes affected the basin formation. The outer and distal northern Vøring Margin represents a series of deep Cretaceous (Træna Basin and Någrind Syncline) and Cretaceous-Paleocene (Hel Graben) sag sub-basins underlain by a significantly thinned continental crust. These sub-basins developed in between structural highs (Utgard, Nyk and Grimm highs) which are underlain by a thicker crust and interpreted as a series of rigid continental blocks ('buffers'). In addition to the regional Late Jurassic-Early Cretaceous rifting events, we found structural evidence of local Neocomian and mid-Cretaceous extensional reactivation affecting the northern segment of the Vøring Basin. During the mid-Late Cretaceous-Paleocene, the extensional axis within the Vøring Basin province migrated sequentially northwestward to the present day continent-ocean 'boundary'. We also show fundamental differences between the volcanic rifted mid-Norwegian margin and non-volcanic (Iberian-type) margins, and how pre-existing structures/tectonics events can shape the evolution and architecture of the margin.

Key words: *NE Atlantic, Vøring Margin, rifting, sedimentary basins, deep crustal structure, Lower Crustal Body, crustal inheritance, potential field modelling, seismic interpretation.*

1. INTRODUCTION

The processes through which continental rifting develops into oceanic rifting is a major challenge in the Earth Sciences. The relationship between continental rifting and magmatism, and the transition from rifting to spreading (e.g. the breakup stage), are still poorly understood and controversial. Important questions usually concern: (1) how much continental extension and thinning of the lithosphere predates the initiation of oceanic rifting (e.g. Lavier and Manatschal, 2006; Van Avendonk et al., 2009; Huismans and Beaumont, 2011; Brune et al., 2016); (2) how the rifting and breakup extension are physically and rheologically accommodated by faulting/shearing and/or igneous additions (e.g. Ebinger and Casey, 2001; Buck, 2006; Yamasaki and Gernigon, 2009; Rosenbaum et al., 2010; Brune et al., 2012); (3) the role of inheritance in rift and drift development (e.g. Harry and Bowling, 1999; Petersen and Schiffer, 2016); and (4) the fundamental magmatic and tectonic differences between "magma-poor" and volcanic rifted margins (Franke et al., 2013; Geoffroy et al., 2015).

In this context, we explore the crustal structure and tectonostratigraphic development of the Vøring Margin which is a part of the mid-Norwegian margin (Figure 1). The Vøring Margin is long recognized to be a classic example of a volcanic rifted margin. It is characterized by a long period of rifting, distal basaltic seaward-dipping reflectors (SDRs), extensive distribution of mafic dikes and sills in the continental crust and sedimentary basins, and the presence of high-velocity (Vp > 7.0 km/s) lower crustal bodies (Eldholm et al., 1989; Planke et al., 1991; Skogseid et al., 2000; Abdelmalak et al., 2015, 2017; Mjelde et al., 2016).

The northern part of the Vøring Margin represents a specific transitional structural domain bounded by two prominent transfer zones – the Surt and Bivrost lineaments (Figure 1a). However, this particular segment of the Vøring Margin was poorly documented and less studied in terms of pre-breakup tectonic evolution and crustal architecture. The main period of data acquisition and interpretation that resulted in the development of the tectonostratigraphic framework of this segment occurred two decades ago. This geophysical and geological material has been reviewed and summarized in the context of regional tectonics (Planke et al., 1991; Skogseid et al., 1992; Blystad et al., 1995; Mjelde et al., 1998; Brekke, 2000; Mosar, 2000; Mosar et al., 2002; Osmundsen et al., 2002; Tsikalas et al., 2008; Lundin and Doré, 2013). Only a few semi-regional case studies focus on and document the Late Cretaceous-Paleocene rifting event preceding the breakup (Ren et al., 1998, 2003; Mogensen et al., 2000; Gernigon et al., 2003; Imber et al., 2005; Fjellanger et al., 2005). Other studies have used published datasets and materials to underpin potential field modelling exercises (Walker et al., 1997; Kusznir et al., 2005; Ebbing et al., 2006; Scheck-Wenderoth et al., 2007; Theissen-Krah & Rupke, 2009; Wangen et al., 2011; Maystrenko et al., 2017).

Various controversial scenarios have been proposed to explain the dynamic and depositional evolution of the Vøring Margin and its associated basins. The most recent studies have suggested some similarities with the Iberian ("magma-poor") type of passive margins (Reynisson et al., 2010; Lundin & Dore, 2011; Rüpke et al., 2013; Peron-Pinvidic and Osmundsen, 2016) implying the presence of relatively wide, serpentinized/exhumed mantle domains in the central, distal and volcanic parts of the margin. In contrast, other publications consider fundamental differences with magma-poor margin (Iberian type) highlighting the role of crustal inheritance and rift duration on passive margin development and showing that there are no clear prerequisites and clear evidence to support a broad zone

of mantle exhumation/serpentinization within the mid-Norwegian margin (Gernigon et al., 2003, 2004, 2015; Nirrengarten et al., 2014; Petersen and Schiffer, 2016; Theissen-Krah et al., 2017; Abdelmalak et al., 2017; Maystrenko et al., 2017). One of the debate concerns the origin and geological interpretation of the strong crustal reflections underlying mostly Cretaceous highs and basins in the distal and outer domains of the margin. This is a key aspect to consider in defining a model of the development of the mid-Norwegian margin and the Vøring segment in particular. A better combination of multidisciplinary geological datasets (refraction and reflection seismic, gravity and magnetic, bio/lithostratigraphy, structural geology, tectonic and potential field modelling, etc.) is therefore necessary to validate both sedimentary and crustal interpretations (see Saltus and Blakely, 2011 for a discussion).

In this contribution, we use new and reprocessed seismic datasets, combined with recently released and revised well biostratigraphy, in order to refine the basin architecture and the Cretaceous-Paleocene tectonic evolution of the northern Vøring Margin. Over the last decade, a new generation of long-offset, high quality seismic reflection profiles covering the entire mid-Norwegian margin has permitted an improvement in the imaging of the deep basin structures and allowed better regional seismic interpretation. Our seismic reflection interpretation is compared with available ocean-bottom seismometers (OBS) data and expanded spread profiles (ESP), and combined with a potential field modelling along a representative NW-SE oriented crustal transect across the northern Vøring Margin. This multidisciplinary approach allow us to evaluate the properties of the deep structures beneath the sedimentary cover and test hypotheses about the style of crustal deformation and sedimentation in a poly-rifted volcanic margin setting. We finally propose and discuss a crustal and tectonic scenario for the rifted margin evolution.

2. REGIONAL SETTING

The present structure of the Vøring Margin off mid-Norway is a result of several post-Caledonian extensional episodes culminating with the complete separation between Norway and Greenland in the earliest Eocene (Talwani and Eldholm, 1977; Brekke, 2000; Faleide et al., 2008). The Vøring Margin can be divided into a series of second-order structures (basins, highs, grabens, etc.; Figure 1a) formed during Late Jurassic-Early Cretaceous and Late Cretaceous-Paleocene rifting (Blystad et al., 1995). Additional extensional events took place in mid-Cretaceous time (Bjørnseth et al., 1997; Lundin and Doré, 1997; Pascoe et al., 1999; Gernigon et al., 2003; Roberts et al., 2009; Tsikalas et al., 2012), but is still a matter of debate because some authors believe that the mid-Cretaceous period was dominantly a quiet tectonic period (Færseth and Lien, 2002; Færseth, 2012). The Late Cretaceous-Paleocene rifting phase, which culminated in continental breakup near the Paleocene-Eocene transition (56 Ma), was associated with extensive and voluminous magmatic activity (Eldholm et al., 2002). This large magmatic event is traditionally correlated with the arrival of the Icelandic mantle 'plume' (Skogseid et al., 2000) and/or independent sub-lithospheric processes (van Wijk et al., 2001; Meyer et al., 2007, Simon et al., 2009; Foulger, 2010).

The post-breakup evolution of the Vøring Margin is characterized mainly by thermal cooling and regional subsidence of the sedimentary basins (Brekke et al., 2000; Faleide et al., 2008). A mid-Cenozoic compressional event is also expressed by a number of inversion structures (domes/arches, reverse faults etc.) which are likely the result of a compressive stress dominantly induced by ridge push (Vågnes et al., 1998; Doré et al., 2008). The final development of the margin is closely linked with northern hemisphere glaciation events, when large Plio-Pleistocene depocenters expanded over the area, increasing the regional

subsidence and tilt of the margin (Hjelstuen et al., 1999; Rise et al., 2005; Faleide et al., 2008).

The northern Vøring Margin segment, which forms the focus of this study, is located west of the Nordland region onshore Norway (Figure 1). The Trøndelag Platform, which defines the proximal part of the margin segment, is a large and shallow platform containing post-Caledonian Late Paleozoic to Late Mesozoic basins (Figures 1 and 4a). The distal and outer parts of the Vøring Basin province are characterized by NE-SW oriented structural basin highs (e.g. the Utgard High, The Nyk High) and deep sub-basins (e.g. the Traena Basin, the Någrind Syncline and the Hel Graben) (Figure 1 and 4a). The Vøring Basin is characterized by the Surt and Bivrost lineaments defined between the adjacent central Vøring Margin segment and the Lofoten Margin to the north (Figure 1). The transition to the outer margin domain is strongly affected by Late Cretaceous-Paleocene extensional deformation within the so-called Grimm-Rym-Nyk structural "ring" which resulted in the formation of the deep Paleocene Hel Graben and the newly defined Hermod Basin (Figure 1). The outer domain is outlined by the Paleocene Hel Terrace and Grimm High, the latter is covered by relatively thin breakup-related volcanic sequences and is interpreted as a deep-seated structural high (Abdelmalak et al., 2016b).

3. DATASET AND METHODS

We interpreted a large set of high-quality seismic reflection lines acquired and processed by TGS (Figure 1b). The seismic data is time migrated with a positive amplitude at the sea bed, and is of good to excellent quality, although some deterioration occurs below sill intrusions. The potential field data was provided and processed by TGS. Well formation tops were obtained from the Norwegian Petroleum Directorate (NPD) (NPD factpages, 2017) and

the Norwegian Offshore Stratigraphic Lexicon (NORLEX) group (Gradstein et al., 2010). The raw results of biostratigraphic analyses and wireline logs for well 6608/2-1S have been provided by the NPD but have been re-evaluated by RPS Ichron (see appendix 1 and figure A1).

The seismic dataset has been jointly interpreted together with potential field data (Figure 2) and published crustal-scale velocity data (Figure 1b) derived from Ocean Basin Seismometer (OBS) and Expanded Spread Profiles (EPS) surveys (Planke et al., 1991; Digranes et al., 1996; Mjelde et al., 1998).

3.1. Seismic interpretation

The regional seismic interpretation has been carried out using IHS Kingdom software. The line spacing of the final dataset (Figure 1b) ranges from 0.2 to 2 km, which was sufficient enough to confidently tie the different seismic units mapped in this study. We interpreted a set of regional Cretaceous-early Cenozoic seismic horizons over the entire northern Vøring Margin (Figure 3). These units were correlated with the well database. The final regional horizons include: the Base Cretaceous Unconformity (BCU), mid-Albian (?) (MA), mid-Cenomanian (MC), Top Turonian (TT), intra mid-Campanian (IMC), the Base Tertiary Unconformity (BT) and Top Paleocene (TP) (Figure 3). Additionally, several pre-Cretaceous reflections were picked on the Trøndelag Platform, while Top Santonian (TS) and Base Late Pliocene (BLP) have been interpreted locally. We constructed a number of time-thickness (isochore) maps (Figure 11) in order to highlight the regional configuration of the main depocentres, their migration through time and space, and their relationship with the deep crustal architecture of the margin.

The crustal structure for the proximal part (Trøndelag Platform) was obtained from the reflection data where the interpreted top crystalline basement (TB) marker can be reliably identified over the area and tied with wells. To further constrain the crustal structure of the deep Vøring Basin we compared the seismic interpretation with the top basement grid from an available 3D lithospheric model (previously published by Scheck-Wenderoth and Maystrenko, (2011)). In the areas where the top basement grid crosses confidently interpreted sedimentary successions, we moved it down to a depth level consistent with the seismic observation since the new and reprocessed long-offset seismic data allow us now to more confidently identify deeper strong mid-crustal reflections in the sedimentary basin. Most likely deeper than 10-11 s TWT, the Moho is barely recognized on the seismic reflection data; as a result, we used OBS and ESP data and potential field modelling results to identify and map the Moho.

3.2. Potential field data

The 50-km high-pass filtered Bouguer gravity anomaly map processed by TGS (Figure 2a) reveals a complex pattern of high- and low-amplitude anomalies along the margin. High-pass filtering of the data makes it possible to dissociate gravity anomalies caused by shallow basement structures from density variations from the deepest crust and/or the upper mantle. Cut-off wavelengths of 50 km emphasize density contrasts with source depth usually deeper than 10 km.

50-km high-pass filtered magnetic data (Figure 2b) is based on the Mid-Norway Aeromagnetic Compilation (MNAM) compilation by TGS, including the most recent ship track-and aeromagnetic surveys in the Vøring margin. Within the continental domain, these data allowed identification of the main deep-sourced magnetic anomalies. It provides

information about the deep continental basement rocks expected below the non-magnetic sedimentary cover. 50-km high-pass filtered potential field data were included in the seismic project, scaled to two-way travel time, converted to pseudo-horizons and displayed on the seismic lines to facilitate the joint interpretation of the seismic, gravity and magnetic data.

3.3. Potential field modelling of the northern Vøring transect

Potential field modelling is a useful technique to evaluate and check further basement depth, nature and properties. To illustrate the crustal configuration of the northern Vøring Margin, a 2D potential field modelling has been carried out along a characteristic NW-SE section striking from the Helgeland Basin on the Trøndelag Platform up to the continent-ocean 'boundary' (Figure 4). This section illustrates the main crustal configuration interpreted beneath the main structural highs and sub-basins described in this study. The forward modelling has been carried out using the commercial software GM-SYS integrated within the GEOSOFT Oasis Montaj software. The modelling itself is based on the conventional and original method of Talwani (1973), where sets of irregular polygons with different physical properties along a 2D transect calculate magnetic and gravity signals that are then compared with the observed potential field values. The geometry and properties of the polygons are changed accordingly until the best fit between the observed and calculated signal is achieved.

The 2D margin transect was first depth-converted using hiQbe™ Mid-Norway, a regional high-quality seismic velocity cube covering the entire mid-Norwegian margin (http://www.first-geo.com/products/hiqbe/norway). The velocity cube has been compiled from 536 seismic stacking velocity datasets, including the stacking velocities along the transect, employing proprietary and industry standard geostatistical methods. The stacking velocities are calibrated to 230 check shots from wells, compensating for delta anisotropy – a parameter

describing the near vertical P-wave propagation (Thomsen, 1986). At depths below well control, the delta anisotropy cannot be calculated directly from the well check-shot. Calibration was then achieved by extrapolating the delta anisotropy downwards in such a way that the hiQbe™ velocities are comparable to those derived from seismic refraction modelling of OBS-data (e.g., Ní Dheasúna et al., 2012).

The software TecMod 2D was also used to estimate total and tectonic subsidence rates for a series of rifting episodes in the Træna Basin calculated with forward modelling and classic backstripping approach. Kinematic, isostatic and thermal principles of these approaches and their comparison are described in detail by Rüpke et al. (2008, 2010), Theissen-Krah and Rüpke (2009) and Clark et al. (2014).

4. RESULTS

4.1. Geological structure, seismic interpretation and correlation with potential field data along the transect

Transect on figure 4a illustrates the main basin and structural configuration of the northern Vøring Margin. The 342 km long transect strikes NW-SE from the Ylvingen Fault Zone at the Helgeland Basin on the Trøndelag Platform across the Vøring Basin and terminates close to the expected continent-ocean 'boundary'.

The Trøndelag Platform defines the proximal and shallower part of the margin segment and shows Devonian-Early Carboniferous? to Jurassic basins (Blystad et al., 1995; Osmundsen et al., 2002) bounded to the east by the Caledonian basement that crops out in the onshore part. The structure of the thick Late Paleozoic basin (up to 6 km) is dominantly controlled by fault systems (Figure 4) which was possibly initiated during post-Caledonian

orogenic collapse, and then sequentially reactivated during Carboniferous?-Permian rifting episodes (e.g. Doré et al., 1999). To the west, this Paleozoic basin extends to a prominent basement horst lying at the northern prolongation of the Nordland Ridge (Figures 1a and 4a). Due to high density, this basement horst coincides with a pronounced gravity anomaly observed at that level (Figures 2b and 4b). We were able to tie a top basement marker to well 6609/7-1 where this horst structure was drilled and basement rocks were reached at a shallow level of 1912 m (NPD factpages, 2017). The recovered rocks predominantly consist of pre-Cambrian quartzite and other low-medium grade metamorphic rocks with evident sedimentary origin (Slagstad et al., 2011).

Later Mesozoic faulting activity in the area generated second order half-grabens, grabens and horst structures. Triassic to Jurassic sediments covered the deep Late Paleozoic basin and the basement horst and were subsequently peneplained in the Nordland Ridge at the BCU level. The superimposed Helgeland Basin (Figure 4a) observed in the inner platform contains a mainly Early Cretaceous sedimentary fill (Blystad et al., 1995; Brekke, 2000).

Our seismic interpretation shows basinward-dipping fault systems at the north-western flank of the Nordland Ridge/Grønøy High (Figure 5). Those faults controlled the Cretaceous evolution of the narrow and deep Træna Basin, which was poorly imaged by the previous seismic datasets. Compared to surroundings, the Træna Basin is characterized by NE-trending negative gravity and magnetic anomalies (Figure 2a-b). Despite a uniformly deep configuration of the basin along its strike, we observed a subtle increase of the magnetic and gravity signal (Figure 2a-b) towards the Lofoten-Vesterålen Margin which coincides with a strong seismic reflection underlying the deep-seated pre-Cretaceous fault blocks (Figure 5). The transition to the adjacent deep Rås Basin is marked by prominent N-trending, relatively strong, positive gravity and magnetic anomalies (Figure 2a-b and 5) lying in the prolongation of the Surt Lineament, which is interpreted as an old inherited basement structure (Blystad et

al., 1995). Our interpretation highlights a deep basin configuration (BCU at 7-8 s in the axial part; figure 5). Regional mapping and our revised calibration suggest thin Lower Cretaceous successions (about 1 s TWT) underlying thick Coniacian to mid-Campanian sequences (Figure 5)

The northwestern flank of the Træna Basin is defined by the Utgard High. This prominent basement high, which is characterized by a strong NE-trending gravity anomaly, can be divided into two segments (Figure 2a). The gravity anomaly is clearly connected to a prominent high-amplitude reflection observed in the deep part of the high (Figure 6a-d). We have to note here that the observed reflection represents some deep local features but we were not able to establish any direct and spatial connection with the notable and similar deep *T*-Reflection defined and described further west in the outer part of the Vøring Basin (see Gernigon et al., 2003; Abdelmalak et al., 2017). In this study, we named it as the *UH* (Utgard High)-Reflection to specify the difference from the *T*-Reflection. In the southern segment of the Utgard High, the *UH*-Reflection shows a gently undulating configuration at a relatively deep level (7.5-8 s TWT) (Figure 6a-b). In the northern segment the *UH*-Reflection shallows up to 5 s TWT, where it fits well with a stronger gravity signal (Figure 6c-d). In its shallow part, the *UH*-Reflection is disrupted and displaced both by a series of Late Jurassic-Early Cretaceous (and older?) and Late Cretaceous-Paleocene landward–dipping normal fault systems (Figure 6b, d) that control the structural development of the Utgard High (Skogseid et al., 1992; Blystad et al., 1995).

The recent drilling results (well 6608/2-1S) in the northern Utgard High indicated that the BCU is much deeper than was previously thought (Blystad et al., 1995; Brekke, 2000), with sediments from the Lower Cretaceous Lyr Formation still preserved at the well bottom (5.6 km; see appendix 1). Accordingly, we could not expect much pre-Cretaceous sediments in the northern Utgard High (1-1.5 km thick) if we assume the potential basement

origin of the *UH*-Reflection (see also modelling results and discussion). Furthermore, our biostratigraphic reinterpretation of well 6608/2-1S (see appendix 1 and figure A1) suggests a significant thickness of the Lower Cretaceous sediments (>1.1 km) and a thinner Turonian interval in comparison to the previous interpretations (Blystad et al., 1995; Brekke, 2000). The Turonian interval of the well is considered to be either condensed or representative of a stratigraphic unconformity. Our biostratigraphic analysis of well 6608/2-1S confirms the presence of Middle-Late Turonian biomarkers but also suggests a lack of Early Turonian assemblages. Tentatively, we explain the lack of early Turonian biomarkers by the presence of an unconformity within the early and partly middle Turonian intervals apparently missing from the section.

Further to the northwest, the Utgard High flanks the Någrind Syncline, a 10 km thick deep Cretaceous sag-basin better imaged now with the new seismic data (Figure 7). The Surt Lineament separates the Någrind Syncline from the Vigrid Syncline in the south-west, whereas its northern continuation is limited by the Bivrost Lineament (Figure 1a). Like the Træna Basin, the Någrind Syncline also corresponds to strong negative gravity and magnetic anomalies (Figure 2a-b). The tectonic history of the Någrind Syncline is strongly related to the Late Jurassic to Paleocene development of the adjacent highs (the Nyk and Utgard highs) and the structural evolution of the flanking/bounding transfer zones (e.g. the Surt and Bivrost Lineaments; Blystad et al., 1995; Brekke, 2000). We found evidence that the Jurassic-early Cretaceous rifting did not terminate here at BCU level (Berriasian; Dalland et al., 1988), but prolongated into the Neocomian (Barremian-Aptian?) time. The early and late syn-rift wedges of Jurassic-Early Cretaceous and possible Neocomian age respectively were controlled by normal faulting on the flanks of a deep basement horst lying below the Nyk High (Figure 7).

The nearly NE-trending positive gravity and magnetic trend in the Nyk High correlates well with a shallow basement high observed at that level (Figure 2a-b). The anomalies curve in an almost southern direction within the Surt Lineament mimicking the deep structural configuration. The dominant and shallower structural style of the Nyk High at the present-day represents the uplifted and eroded footwall of a rifting system, which initiated in Late Cretaceous time and was active during most of the Paleocene (Mogensen et al., 2000; Gernigon et al., 2003; Ren et al., 2003). Rift shoulder uplift of the Nyk High was concomitant with a significant subsidence of the adjacent Någrind Syncline, which is not particularly affected by classic rotated fault blocks. The ongoing extension during the Paleocene promoted severe collapse of the western flank of the Nyk High, thus creating significant accommodation space resulting in preservation of a thick Paleocene succession observed and drilled (e.g. well 6706/6-1) in the Hel Graben (Figure 4a). Later Paleocene-early Eocene minor sinistral transpressional reactivation complicated the fault pattern within the Nyk High (Imber et al., 2005).

There is still an ongoing debate on the Late Cretaceous-Paleocene development of the Hel Graben. The more recent interpretations rely on the controversial stratigraphic analysis of well 6706/6-1. The NPD claims there is at least 1400 m of Paleocene deposits in the well (NPD factpages, 2017) with no penetration within Upper Cretaceous sediments expected at that level in pre-drilling interpretation (Blystad et al., 1995; Ren et al., 2003). In contrast, the NORLEX team (Gradstein et al., 2010 and well report at http://www.nhm.uio.no/norlex) interprets the same section as comprising Upper Cretaceous Shetland Group sediments, suggesting only 200 meters of Paleocene sediments in the well; this interpretation implies that the Hel Graben is dominantly a Late Cretaceous rather than Paleocene syn-rift feature (e.g. Fjellanger et al., 2005). Our own seismic tie from the adjacent Vigrid Syncline into the Hel Graben across the Rym Fault Zone (Figure 8) does support the

presence of thick Paleocene sediments in the Hel Graben. However, our interpretation of the deepest parts of the structure is less confident due to poor imaging caused by extensive distribution of magmatic intrusives, making our assessment of the pre-Paleocene structure more speculative. However, seismic imaging locally allows to estimate the relative depth of the BCU (Figure 8).

The Hel Graben is characterized by a rounded negative gravity anomaly (Figure 2a). It laterally passes into the Paleocene Hermod Basin interpreted as a separate sub-basin in this study (Figures 1a and 8). The limit between the two sub-basins is characterized by a deep-seated high (Figure 8). The gravity pattern shows that the Hermod Basin may extend northeast towards the outer Lofoten Margin (Figure 2a) and possibly merge with the Røst Basin as recently suggested by Maystrenko et al. (2017). The 3D potential field modelling of Maystrenko et al. (2017) suggests that thick Late Cretaceous-Paleocene sequences (undifferentiated) may likely exist underneath the Lofoten lava inner flows.

The northern boundary of the Hel Graben is defined by the Hel Terrace. Together with the Hermod Basin this is also a newly defined structural element. It is characterized by a series of southward-dipping Late Cretaceous-Paleocene growth faults (Figure 9a) possibly decoupled and developing over overpressured mobile shales widely distributed in Lower to mid-Cretaceous intervals in the deep Vøring Basin (Dalland et al., 1988; Brekke et al., 1999; Vergara et al., 2001). Further northeast, the northern flank of the Hel Terrace is characterized by a graben-like feature with clear syn-rift Paleocene seismic wedges postdating the main Late Cretaceous-Paleocene extensional phase leading to the formation of the Hel Graben (Figure 9b). The new seismic data also suggest that the footwall of the Hel Terrace was also exposed and peneplained during this period. Notably, we discovered evidence of earlier pulses of magmatism (intra-Paleocene) in the Hermod Basin compared to the main Early Eocene volcanic event recognized in the Vøring Marginal High. This early phase of

magmatism is witnessed by older vent complexes that developed in the Paleocene successions and genetically linked with deeper sill intrusions (Figure 9b). Later mid-Miocene and Plio-Pleistocene inversion also shaped the Hel Graben and partly the Hel Terrace to form the wide Naglfar Dome (Figure 8, 9a-b).

The sub-basalt Grimm High (Figures 4 and 10) has been defined based on a previous integrated seismic-gravity-magnetic interpretation of the volcanic margin (Abdelmalak et al., 2016b). It coincides with a gravity high that correlates with a positive magnetic anomaly, suggesting a shallow basement beneath the basalt (Figure 2a-b and 10). The anomalies also correlate well with a structural high interpreted at the top and base basalt levels at the Vøring Marginal High (Abdelmalak et al., 2016b). The Grimm High has a thin basaltic cover (Abdelmalak et al., 2016b), reflecting its relatively high elevation when subaerial volcanic sequences were deposited in the earliest Eocene. Notably the gravity high observed at that level also fits a high-amplitude reflection observed at 15 km in the deep part of the Grimm High (Figures 4a, b and 10). The deep reflection coincides spatially with the deep and faulted *T*-Reflection described and defined in the outer Vøring Basin (Gernigon et al., 2003, 2004; Abdelmalak et al., 2017). At the level of the Grimm High, the new seismic data revealed tilted fault block system below the volcanics (Figure 10), with a structural style similar to that observed in the adjacent North Gjallar Ridge (Gernigon et al., 2003, 2004; Ren et al., 2003). The upper syn-rift feature could represent the equivalent of the Campanian-Maastrichtian Springar Formation penetrated by well 6704/12-1 in the North Gjallar Ridge (Gernigon et al., 2003; Fjellanger et al., 2005).

4.2. Regional development of the main Cretaceous-Paleocene tectonostratigraphic units

Having described the present margin geometry, we here infer its evolution based on different isochore maps (Figure 11a-f). We organize this from oldest to youngest, focusing on thickness trends and onlap patterns around major sub-basins and flanking structural highs.

Unit K10 (Valanginian to mid-Albian)

The Valanginian to mid-Albian sequence K10 defined in this study is rather reinterpreted as a syn-thinning sequence and not a post-rift as suggested in previous publications (Vergara et al., 2001; Faerseth et al., 2002). The isolated rounded depocentre in the Någrind Syncline reflects the Neocomian (Barremian-Aptian?) faulting/rifting activity observed on the eastern flank of the Nyk High (Figures7 and 11a). However no prominent and concomitant depocentre is identified within the Træna Basin (Figure 11a). The strata of the K10 sequences onlaps the deep terraces imaged in the southern part of the Træna Basin and along the northwestern flank of the Nordland Ridge which was already an elevated feature at that time (Figure 11a). The uplift of the Nordland Ridge was also associated with lateral subsidence of and sedimentation within the Helgeland Basin, which tends to deepen in the northeastern direction (Figure 11a). As previously interpreted (Blystad et al., 1995; Brekke, 2000), the lower Cretaceous succession thins towards the Utgard High, suggesting that a local and central horst configuration was already in a high position at the early stage of the Vøring Margin formation. Slight thinning and local absence of the K10 sequence on top of the Utgard High is confirmed by our seismic observations (Figure 6a-d, 11a). Nevertheless, rather thick lower Cretaceous sediments are also confirmed by well 6008/2-1S

on top the Utgard High. This reflects a complex structural topography in the early stages of the high formation.

The absence and thinning of the Valanginian to mid-Albian K10 sequence in the southern and central Nyk High suggests NE striking basement/BCU highs which were already emerged at that time. Several minor depocentres are observed at the transition between the North Træna Basin and the adjacent Lofoten-Vesterålen Margin (Figure 11a).

Unit K20 (Mid-Albian to mid-Cenomanian)

Similar depositional pattern can be deduced from the mid-Albian to mid-Cenomanian isochore map (unit K20, figure 11b). Clear erosion is seen on the Nordland Ridge and partly on the deep terraces mapped in the southeastern part of the Træna Basin (Figure 11b). According to the sediment thickness distribution, the Træna Basin was still characterized by a slow sedimentation rate during the K20 deposition. Thinning of the sequence K20 is also interpreted towards the Utgard High (Figure 11b). However, locally poor quality of seismic imaging there makes such conclusions a bit uncertain. We identified several scattered depocentres blanketing the Någrind Syncline, and its transition to the Vigrid Syncline and partly the Nyk High (Figure 11b). We also observe significant thickening of the K20 at the transition between the Någrind Syncline and the Lofoten-Vesterålen Margin.

Unit K30 (Mid-Cenomanian-Early Coniacian)

Deposition of the mid-Cenomanian-Early Coniacian unit K30 mainly occurred in the Træna Basin, which defined a deep (up to 1.7 s TWT), prominent and NE-SW elongated (100×25 km), fault-controlled depocentre that deepened towards the southern Rås Basin (Figure 11c). The depocentre-related fault tended to develop over reactivated fault systems observed on both flanks of the Cretaceous sub-sag basin (Figure 4a). Both seismic observations and isochores indicate that the syn-thinning subsidence shifted NE-ward from the Rås Basin. During the same period, a large and relatively thick rounded depocentre (55×45 km; up to 1-1.5 s TWT thick) developed in the adjacent Någrind Syncline. Thinning of the K30 unit is observed on the SE-flank of the North Gjallar Ridge and in the Utgard Ridge, indicating their relatively high structural position during this period (Figure 11c).

Unit K40 (Coniacian to mid-Campanian)

Rapid subsidence and accommodation of a large, NW-SE elongated (150×30km) thick depocentre (up to 2.9 s TWT or 6 km thick) during the Coniacian to mid-Campanian K40 period (Figure 11d) concentrated in the Træna Basin. Based on seismic observations, we suggest that fault-driven tectonic subsidence ceased around Santonian and then the Træna Basin was passively infilled during the early to mid-Campanian. Thinning and erosion of the K40 unit on both flanks of the Utgard High confirm its shallow bathymetric configuration at that period (Figure 11d). Rather high sediment accumulation rates persisted along the axis of the Någrind Syncline with the deposition of the Nise Formation sourced from NE Greenland (Morton and Grant, 1998). In the Campanian, the North Gjallar Ridge was still in a relative high position and shallow marine setting as illustrated by the absence and/or pinch out of the

K40 unit on its SE-flank as confirmed by well 6705/10-1 (Asterix). Furthermore, thinning of the unit K40 towards the Hel Terrace (Figure 11d) also indicates a shallower structure in that domain.

Unit K50 (Mid-Campanian to Base Tertiary)

A dramatic depocentre shift of the unit K50 occurred from the mid-Campanian to the beginning of the Tertiary (e.g. the Base Tertiary Unconformity). The main sedimentation axis moved NW-ward from the Træna Basin to the Någrind Syncline (Figure 9e). The depocentre shape mimics the pre-existing basin configuration developing in between deep-seated structural highs (Figure 11e). In the SW Någrind Syncline and its transition to the Vigrid Syncline, the depocentre is seemingly not fault-controlled. However, subsidence and higher sedimentation in the NE segment of the Någrind Syncline could be enhanced by additional reactivation of the SE-dipping faults locally observed on the flank of the adjacent Nyk High (Figure 4a). The sequence K50 is thinned significantly along the Nyk High and the North Gjallar Ridge, which were both uplifted during this period. Smaller thicknesses of K50 are also observed on the Utgard High. Notably, the Hel Terrace was still in a shallower position with K50 onlaps onto its southern flank, suggesting a structural evolution quite similar to the adjacent North Gjallar Ridge.

Unit P10 (Paleocene)

Another marked change in sedimentation pattern happened during deposition of sequence P10 in Paleocene, when the depocentre suddenly migrated north-westward towards the Hel Graben and the Hermod Basin (Figure 11f). In the central part of the outer Vøring Basin, faulting migrated progressively towards the volcanic domain growing at the same period (Gernigon et al., 2004). On the NW flank of the Nyk High, deposition and subsidence was controlled by collapse, facilitated by slip along the pre-existing Rym Fault Zone. Additional evidence for later Paleocene faulting/rifting is seen in the northern part of the basin (e.g. the Hel Terrace) (Figure 9a-b).

Minor depocentres in the Vigrid/Någrind syncline axis and near the Lofoten-Vesterålen Margin (Figures 7 and 11f) are not fault-controlled; instead they are likely interpreted as sedimentary bodies (e.g. fans) sourced from the neighboring eroded highs. Erosion of the sequence P10 in the Utgard High is possibly the result of late stages of subsequent Early Tertiary strike-slip reactivation along the Fles Fault Complex as previously noted by Blystad et al. (1995).

4.3. Potential field modelling of the regional transect and crustal configuration

The 2D forward potential field modelling of the northern Vøring transect (Figure 4a-b) was carried out to better constrain the crustal architecture and basement properties underlying the complex depocentre system previously described in this study. The initial crustal parameters used in the potential field modelling are shown in the table 1 (see also Appendix 2).

While the Moho configuration in the Trøndelag Platform is constrained by several ESPs (Planke et al., 1991), depth of top basement was entirely obtained from the new seismic

reflection data, where the expected top basement surface represents a well-defined seismic marker. The total crustal thickness decreases down to 10 km in the axial part of the platform, where we have to presume attenuated upper to lower crust and exhumation of the high density, lower crustal body (3100 kg/m^3) at 15 km depth; an interpretation consistent with the high velocities (around 7.1 km/s) and depth estimations taken from the available ESP data (Planke et al., 1991).

The transition zone to the Træna Basin corresponds to an abrupt thinning of the continental crust over less than 40 km from thickness in 18 km at the Nordland Ridge to 4-5 km in the central axis of the Traena Basin (Figure 4b). As suggested by Maystrenko et al. (2017), the first necking of the rift system is located in this position. The Moho shallows from 25 km to 20 km in the Utgard-Træna area (Planke et al., 1991; Mjelde et al., 1998).

The northern Utgard High forms the most prominent magnetic and gravity signals along the profile (Figure 4b). In order to fit the prominent gravity signature and surrounding refraction data, we assumed a thick (10-12 km), ultra-high-density body (ULCB) (3200 kg/m^3) from Moho level to relatively shallow position (8-10 km) in the lower and upper part of the crust. Based on our modelling results, we have to assume 1 km thick mid-crustal lenses, which are most likely preserved on both flanks of the structure and almost in contact with the metasedimentary pre- and syn-rift rocks. According to our seismic observations the top of the ULCB deduced from potential field modelling correlates well with the *UH*-Reflection (Figures 4b and 6d) implying a significant impedance (density/velocity) contrast at that level. The basement below the Træna Basin necessitates massive and very high density and magnetic rocks (Figure 4b). Our modelling results do not support the presence and/or preservation of deeper Mesozoic sedimentary rocks in depth. Accordingly, we suppose that the thin and ultra-high density lower continental crust may directly underlie the basin possibly coinciding with

the strong reflection and possible contact observed within pre-Cretaceous fault blocks (Figure 5).

A minimum crustal thickness of 5-6 km in the deep-sag Någrind Syncline is expected at the connection to the NW flank of the Utgard High (Figure 4b). The top of the basement is reliably defined in reflection seismic and correlative with refraction data lying at 13 km at the cross-point with OBS line 7-96 (Mjelde et al., 1998). The basement shallows to 7.5 km towards the Nyk High and forms a prominent paleo-high with total crustal thickness in 13-15 km also confirmed by OBS line 7-96 (Mjelde et al., 1998) and ESP data (Planke et al., 1991). Lens-shaped bodies of middle, lower crust and a dense LCB (1 to 3 km thick apiece) are required there to fit the observed potential field data.

The axial part of the Hel Graben is not crossed by any refraction profiles (Figure 2b and 4b). We modeled the Moho rises to 18 km depth which corresponds to a drastic thinning of the crust reduced to 3-4 km thick in the central part of the Hel Graben. Since we believed that the BCU was confidently interpreted at the position of the transect, we made structural corrections for the pre-Cretaceous configuration in the central Hel Graben (Figure 4a). Based on our modelling, we had to agree on extremely thin or no pre-Cretaceous sediments below this unconformity in order to get a better fit with the observed gravity (Figure 4b). As a result, the Cretaceous sediments most likely lie directly on top of a high density lower crust also expected in the central part of the Hel Graben (Figure 4b). This crustal configuration also implies that upper to lower crust is most likely substantially delaminated or absent there. The presence of pre-Cretaceous sediments is not totally excluded but if present, these metamorphosed sequences are extremely compacted and/or highly deformed. With realistic magnetic susceptibility values in the basement, we have not been able to reach a solid fit with the observed magnetic anomalies at the Hel Graben (Figure 4b). This discrepancy could be

explained by the magnetic influence of the large shallow sill complex observed in the Hel Graben (e.g. Berndt et al., 2000) and is not considered in this paper.

Presence of the deep-seated continental basement block underneath the Vøring Marginal High within the sub-basalt Grimm High (Abdelmalak et al., 2016b) is in agreement with our modelling results (Figure 4b). A crustal fragment with a thickness of more than 10 km is expected there. The Moho beneath the Grimm High is also relatively well constrained at 25 km from previous OBS and ESP data (Planke et al., 1991; Mjelde et al., 1997, 1998) and then shallows to less than 20 km towards the continent-ocean 'boundary'. The prolongation of the *T*-Reflection expected at that level partly corresponds to the boundary between the lower crust and the LCB bodies modeled in the distal part of the transect (Figure 4a, b). To fit the gravity, our model also suggests that up to 3 km of pre-Cretaceous strata could be preserved above the continental basement expected underneath the basalt.

5. DISCUSSION

5.1. Origin and geophysical properties of the Lower Crustal Bodies (LCBs)

Origin of the Utgard ultra-high-density body (ULCB)

Below the Utgard High our modelling suggests the presence of an up to 12 km thick, ultra-high-density (3.2 g/cm^3) lower crustal body (Figure 4b), the top of which is located almost at the level of the *UH*-Reflection. The shallowing of the *UH*-Reflection in the central and northern parts of the Utgard High fits well with the main magnetic and gravity signals (Figure 6c, d). The nature of these potential field anomalies has been extensively discussed. Earlier models (Planke et al., 1991; Skogseid et al., 1992) speculated on the crustal origin of

the anomaly, implying it most likely represents an old, Caledonian, high-density basement block with Mesozoic or pre-Mesozoic age of emplacement. Our observation shows (Figure 6c, d) that the *UH*-Reflection corresponds to the top of the local LCB and has been affected by a series of Mesozoic (and older?) faulting events. Consequently, we also considered that the Utgard High LCB (or part of it) is most likely an inherited basement structure.

Mjelde et al. (2013, 2016) also proposed that the basement here partly consists of lower crustal eclogites with a density of up to 3500 kg/m^3. These eclogites may be related to a sliver of the Caledonian suture zone (e.g. Petersen and Schiffer, 2016). In a recent 3D lithospheric model of the Lofoten-Vesterålen margin and adjacent parts of the Vøring Margin, a thick high-density lower crustal layer of Caledonian origin, with high densities varying from 2985 kg/m^3 to 3070 kg/m^3 has also been considered beneath the Utgard High (Maystrenko et al., 2017).

Reynisson et al. (2010), based on their regional 3D potential field modelling, interpreted part of the LCB within the Utgard High as heavily (and syn-rift) serpentinized mantle, assuming very thin crust underneath the high. Our modelling and observations suggest, however, that the Utgard High was an old crustal horst partly shielded from drastic thinning (Figure 12), compared to the surrounding sub-basins (e.g. Traena Basin and Nagrind Basin). The clear correlation with the central horst system acting as a thick tectonic 'buffer' since the early stage of rifting in the northern Vøring Margin suggests that the high-density rock were most likely part of the pre-rift basement even before the onset of drastic thinning of the crust. Wangen et al. (2011) also got unrealistic rates of extension in their tectonic modelling run with a shallow and thin crust at the position of the Utgard High. Therefore, we suggest that the nature of the anomaly is better regarded as a remnant of old Caledonian or Precambrian high-density crustal blocks. Speculative serpentinization within the Utgard High is unlikely for us. This system of crustal blocks may extend towards the Lofoten-Vesterålen

Margin and merge either with the Lofoten Ridge or the Røst High, which are also expressed as prominent, elongated, positive gravity anomalies. It is likely that the anomaly could also be amplified by significant intrusion of breakup-related, high-velocity, dolerite sills (>7.0 km/s) as suggested by Berndt et al. (2000) and Neumann et al. (2013). The density expected at the level of the ULCB is so high (3200 kg/cm^3) and so massive that we disregarded the possibility of preserved deep sediments at that level. This is in contradiction with recent alternative assumptions from Osmundsen et al. (2016). Shallow magnetic source estimations (Fig. 4b) also support the presence of magnetic (basement) rock at 10-15 km and accordingly cannot easily explain the presence of Mesozoic sediments at that level.

Outer LCB

To fit both the observed gravity and the high velocities also deduced from ESP and OBS data, our modelling also requires a high-density LCB (3100 kg/cm^3) in the outer part of the northern Vøring Basin and below the Grimm High (Figure 4b). This body is typically characterized by Vp velocities between 7.1 and 7.7 km/s (Mjelde et al., 2003). The nature of outer LCBs located along continent-ocean 'boundary' has been widely discussed by many authors in the past. Earlier schemes suggest LCB in the distal part of the mid-Norwegian margin represented mafic crust underplated during continental breakup (e.g. White and McKenzie, 1989). However later studies promoted a variety of alternatives on the origin and properties of LCB, ranging from high-velocity intrusions into the lower crust (White et al., 2008; White et al., 2010), heavily serpentinized/exhumed mantle (Ren et al., 1998; Osmundsen and Ebbing, 2008; Reynisson et al., 2010; Peron-Pinvidic and Osmundsen, 2016) and/or a retrograde/high-grade Caledonian lower crust (Gernigon et al., 2004; Ebbing et al., 2006; Mjelde et al., 2016; Petersen and Schiffer, 2016; Abdelmalak et al., 2017).

According to our modelling results (Figure 4b) and new observations (Figure 10), the upper boundary of the outer LCB coincides partly with the sub-basalt prolongation of the *T*-Reflection located at approximately 15 km depth. This high-amplitude reflection also correlates with a strong gravity signal within the Grimm High (Figure 2a). Similar high-amplitude reflection has been earlier described and mapped within the South and North Gjallar Ridges (Gernigon et al., 2003, 2004), where it is also interpreted as a part of an old (possibly Caledonian) inherited piece of lower crust (Gernigon et al., 2004; Ebbing et al., 2006). The *T*-Reflection influenced the basin evolution long before the onset of the breakup magmatism and as early as the initiation of Late Cretaceous-Paleocene rifting in the mid-Late Campanian (Gernigon et al., 2003, 2004). Furthermore, in the recent study by Abdelmalak et al. (2017), the *T*-Reflection in the Hel Graben was also interpreted as the top of LCB, where it coincides with lower crustal sill intrusions and detachment faults. An alternative interpretation of the pre-breakup emplacement of this LCB may also be explained in terms of serpentinization model in the North Gjallar Ridge (Ren et al., 1998). However, sea water penetration into the mantle could not be easily explained if we consider the thick (8-9 km) pre-breakup sedimentary package and the associated decoupled fault system overlying the deep LCB (Figure 10). Thus, in our model we agree that an inherited crustal origin of the LCB is most likely for this distal part of the margin.

5.2 Basin evolution and crustal deformation

Træna Basin Revisited: too narrow and deep to be just a post-rift Cretaceous sag basin?

Very few papers have described the Traena Basin in detail (Blystad et al., 1995; Osmundsen et al., 2002; Gomez et al., 2004). According to Osmundsen et al. (2002), the Træna Basin represents a large rollover structure controlled by an east-dipping detachment fault along the southeast side of the Utgard High which influenced the subsidence of the basin and the formation of two large lower and upper Cretaceous depocentres. In contrast, Gomez et al. (2004) proposed that the Traena Basin was rather controlled by a large west-dipping detachment fault defining the NW-flank of the Nordland Ridge, whereas the NW-dipping flexure of the Nordland Ridge was explained by Late Cretaceous, post-rift thermal subsidence. We do not see any evidence for a significant west-dipping detachment faulting at the BCU or deeper level along the flank of the Nordland Ridge and its transition to the Træna Basin. The Træna Basin could be initiated as a half-graben on the flank of the Utgard High in the Jurassic-Early Cretaceous, with the Nordland Ridge being uplifted and peneplained (Brekke and Riis, 1987; Blystad et al., 1995) as a flexural response during this rifting event, as later proposed by Osmundsen et al. (2002). According to our observations, the subsequent formation of the elongate, narrow and extremely thick Upper Cretaceous depocentre of the Træna Basin is fault-controlled on both sides of the basin, but is not only structurally limited to the southeastern side of the Utgard High. Therefore, the existence of an active and persistent west-dipping detachment through the entire thinning history of the Træna Basin is questionable.

The conjugate faults systems observed on both sides of the Træna Basin (Figure 4a) are sealed by Santonian strata and then were moderately reactivated mainly along the Utgard High as a continuation of the Fles Fault Complex in latest Cretaceous-Paleocene times. One could explain this faulting as a simple result of differential compaction during a long period of post-rift thermal sagging of the basin (Færseth and Lien, 2002). However, the backstripped tectonic subsidence curve (Figure 13) calculated for the central part of the Træna Basin shows an abrupt transition to relatively rapid subsidence magnitude (~2.5 km) starting in the mid-Cenomanian (~95 Ma) and ceasing at Santonian (~85 Ma). Such rapid subsidence (Figures 4a, 13), the atypical high rates of sedimentation during this geologically short time period (10myr), and the narrow basin configuration (~20 km wide) cannot be easily explained by a McKenzie-like thermal subsidence model (McKenzie, 1978) invoking uniform and instantaneous pure shear extension. Narrow, small basins and sub-basins characterized by accelerated and short-lived tectonic subsidence (2-4 km in 10 myr) typically form in pull-apart settings where transtensional strike-slip regime is involved (Christie-Blick and Biddle, 1985; Xie and Heller, 2009). Typical strike-slip basins (e.g. Dead Sea Rift, ten Brink and Ben-Avraham, 1989) tend to lengthen rather than widen during ongoing extension. Transtensional regimes also favor much faster and efficient thinning of the crust, which seems to be the case in the Træna Basin according to the very thin crust expected there (Figure 4b). Notably, Early to Late Cretaceous oblique extension and dextral strike-slip have been described in the adjacent Lofoten–Vesterålen Margin (Bergh et al., 2007).

The observed fault systems controlling the mid-Cenomanian-Santonian subsidence in the Træna Basin show relatively steep configuration (Figure 4a). However, direct evidence for both large-scale strike-slip motions (e.g. negative flower structures) is not well imaged along the basin. Furthermore, the backstripped tectonic subsidence rate in 2.5 km is not uncommon for rift basins (Allen and Allen, 2013). The formation of steep-dipping faults in a

narrow rift basin could explain ongoing rapid subsidence even after rift opening had slowed, as is shown in the Rio Grande Rift (van Wijk et al., 2018). In this case, local transtensional reactivation or extension by slip on steep-dipping faults could explain the mid-Cenomanian-Santonian structural evolution of the narrow, deep Træna Basin. Unfortunately our observations and modelling results cannot fully discriminate between the two scenarios. Nonetheless, a local extensional component during the Cenomanian-Santonian thinning of the Træna Basin could be concomitant with the uplift and tilting of the Trøndelag Platform (Brekke, 2000), the Nordland Ridge (Fjellanger et al., 2005), the Lofoten Margin (Henstra et al., 2016) and the Utgard High. Our biostratigraphic study of well 6608/2-1S in the northern Utgard High (see appendix and figure A1 for details) reveals the presence of a significant Turonian hiatus that could be a result of vertical movements linked with this possible thinning event. Mid-Coniacian extensional reactivation along the flanks of the Træna Basin was also assumed in the regional paleobathymetric model by Roberts et al. (2009). However, the authors did not provide any structural examples for that.

In previous publications, the Træna Basin was characterized by a thick (2 s TWT) Lower Cretaceous succession and a Base Cretaceous unconformity lying at approximately 6-7 s TWT (Blystad et al., 1995), shallowing towards the Lofoten Margin. In previous study, Osmundsen et al. (2002) interpreted a BCU at a deeper level (8 s TWT) but also presumed a thick Lower Cretaceous succession (up to 3 s thick TWT). Our interpretation and regional seismic tie consider thinner Lower Cretaceous sediments in the Træna basin (Figures 4a, 5 and 11a). The absence of thick Lower Cretaceous depocentres in the Træna Basin is also in contrast to Vergara et al. (2001), who proposed regional sediment passive infill of inherited rift-related Jurassic lows during the Berriasian to Albian. On the one hand, the Træna Basin could have been a sediment-starved unfilled rift system at this time. However, relatively thick Lower Cretaceous strata are also preserved on top of the Utgard High "crustal buffer" (Figure

6d), which was located in much shallower position at that stage (Figure 11a). Accordingly, we speculate that much thicker Early Cretaceous sediments would have most likely co-existed in the adjacent sub-basin. To explain such an ambiguity, we propose a crustal scenario where pre-Cretaceous and partly pre-mid-Albian successions were most likely deposited in the proto-Træna Basin, but were subsequently drastically stretched during the Late Jurassic-Cretaceous extensional events (Figure 12). Such a mechanism was described onshore in the inverted Northeastern Pyrenean rifted margin (Clerc et al., 2015, 2016) where similar syn-rift basins developed over greatly thinned continental crust with basin floors representing locally exhumed continental lower crust. In such drastic thinning environments, Clerc et al. (2016) show that both pre- and syn-rift sediments can be affected by syn-metamorphic ductile deformation and transported/laminated together with the extended and highly thinned continental crust. This field analogue could most likely apply to the Træna Basin, where the potential field modelling also supports a drastic thinning of the crust just underneath the Cretaceous sediments (Figure 12). The thinned continental crust in the Træna Basin predominantly consists of ultra-high dense material of possibly Caledonian and/or older origin. This crustal body extends and thickens northwest-ward in the prolongation of the seismic and structural grain observed in the deep basement part of the Utgard High. We propose that the upper-middle crust with pre-rift and syn-rift sediments were deformed and largely squeezed and delaminated in the central part of the Træna Basin, during the exhumation of an old lower crust which are almost in contact with the syn-sag sediments. Due to the great depth of the sediments observed in the Traena Basin, metamorphism and associated ductile deformation is a reasonable hypothesis to propose. It may also explain the difficulty to image any consistent seismic packages underneath the BCU. After Late Jurassic-Early Cretaceous rifting, another active phase of crustal thinning renewed in the Træna Basin

and adjacent areas during the mid-Cenomanian-Santonian. This could explain the sudden increase of the subsidence rate suggested by figure 13.

Deformation patterns in the Nyk-Någrind segment and the Hel Graben

Thanks to the new TGS data, we see clear evidence for a separate Neocomian (Barremian-Aptian?) rifting between the Någrind Syncline and the Nyk High (Figures 7 and 11a). This event succeeds the Jurassic-earliest Cretaceous extensional phase particularly well recognized and constrained in the platform area (Blystad et al., 1995; Brekke, 2000). Up to the mid-Cenomanian, post-rift mainly concentrated within the basin low created during the Late-Jurassic-Neocomian (Barremian-Aptian?) extension. From the mid-Cenomanian to Campanian, both increasing subsidence and deposition shifted southeastward (Figure 11b, c). The depocentres appear to be partly controlled by a west-dipping detachment fault along the adjacent flank of the Utgard High (Figure 4a, b). This observation is partly in agreement with Skogseid et al. (1992), who speculated on a similar development of the Utgard High and its surrounding basins. The middle crust and possible pre-Cretaceous pre-/syn-rift sediments in the adjunction to the Utgard High are drastically stretched along the detachment, with the total crustal thickness of 5-6 km (Figure 4b) constrained by our 2D potential field modelling and also in agreement with Maystrenko et al. (2017).

Previous studies (Brekke, 2000; Lundin and Dore, 2011; Lundin et al., 2013) suggest that the folded geometry of the Någrind Syncline is not a result of a thermal subsidence following the Jurassic-Early Cretaceous rifting phase (Doré et al., 1999), but the consequence of a large scale lithospheric folding caused by a modest Maastrichtian regional compression (Bjørnseth et al., 1997; Lundin et al., 2013). Parallel-bedded strata with relatively uniform thickness below the syncline could support this interpretation (Bjørnseth et al., 1997).

However, we argue that after initial subsidence caused by a series of Late Jurassic to Neocomian extensional events, the Någrind Syncline had a "steer's head" basin geometry with slightly increased sedimentation in its central part and sediment thinning towards the adjacent Nyk and Utgard Highs (Figure 11a-f). Such a geometry is typical for basins that experienced thermal subsidence after a stretching episode (White and McKenzie, 1988). Subsequent reshaping of the Någrind Syncline occurred in mid-Campanian-Maastrichtian time, when the rift axis jumped towards the Hel Graben (Figure 11e-f). During this renewed activity, the north-west flank of the Nyk High, started to rise and fault as a rift shoulder. The uplift of the Nyk High (Figures 4a, 5, 11e-f, 12) generated a concomitant tectonic flexure and rapid subsidence in the Någrind Syncline leading to the formation of a deep depocentre (Figure 11e). We, therefore, prefer to attribute the present-day geometry of the Någrind Syncline to extensional processes rather than a compressional buckling as proposed by Lundin et al. (2013).

Furthermore, in the outer Vøring Basin clear extension dominated in the North and South Gjallar Ridges since the mid-Campanian (Ren et al., 2003; Gernigon et al., 2003). This late rifting event is associated with the formation of clear and prominent syn-rift wedges (Spingar Formation) and normal faults partly cut by the Base Tertiary unconformity (Gernigon et al., 2004). We also precise that the presence of a shallowing Turonian (Lysing Formation) across the North Gjallar Ridge and the Fenris Graben (Osmundsen et al., 2002) is not any longer valid since well 6704/12-1 confirms that these syn-rift sediments are dominantly Campanian-Paleocene in age. In contrast to Lundin et al. (2013), we also believe that the main extension phase in the Gjallar Ridge initiated in the mid-Campanian and not Paleocene, where most of the deformation already migrated toward the volcanic province. In the adjacent Vigrid Syncline, as suggested by Kjennerud and Vergara (2005), an increased

sedimentation in the mid-Campanian-Maastrichtian could also be a response to the onset of this rifting phase in the outer Vøring Basin.

Our study shows that the sub-basaltic Grimm High resembles the North Gjallar Ridge. In addition to the faulting shape of the *T*-Reflection, we also define about 8-10 km of possible pre-mid-Campanian sediments capping the reflection (Figure 10), although poorer seismic imaging below volcanics does not allow a more confident interpretation. Similar structural styles (i.e. tilted fault blocks within Cretaceous strata) and nearly synchronous vertical movements within the Grimm High area and the North Gjallar Ridge during Turonian to Maastrichtian times (Figures 3 and 11d-e) suggest they might be parts of the common structural domain at this time.

The nature of the sudden Paleocene collapse of the Hel Graben is still debatable (Lundin et al., 2013). It is clearly associated with the Nyk High hanging wall slipping towards the graben center, but the crustal mechanism responsible for the structure formation remains unclear. Lundin et al. (2002) proposed that the Hel Graben was formed by a Paleocene caldera eruption possibly coeval with igneous activity associated with the extensive intrusion of high-velocity sills, which thus might have taken place prior to breakup time (Berndt et al., 2000). Evidence for older intra-Paleocene sill intrusions are observed in the Hel Graben (Figure 9b) and could support this interpretation, but the size and origin of such a putative caldera remain difficult to explain. Another model (Gernigon et al., 2003) assumed breakup-related magmatism and thinning could provoke lateral flow of a ductile lower crust below the rift zone. This model could similarly explain both Paleocene uplift of the Nyk High and the collapse of the Hel Graben. Later Lundin et al. (2013) proposed several other possibilities including similar crustal delamination and magma withdrawal during chamber deflation (e.g. Pinel and Jaupart, 2005).

Our seismic interpretation and modelling results consider a highly thinned crust (<5 km) below the Cretaceous-Paleocene Hel Graben (Figure 4b, c). We can only restore and constrain evidence of the Late Cretaceous to Late Paleocene rifting/faulting in the Hel Graben and surrounding structures. However, it is possible that the deepest and older Cretaceous sediments rest directly upon the LCB (Figure 4b, c), while mid-upper crust and pre-Cretaceous pre-/syn- rift deposits (if they still exist) were totally delaminated and/or boudined in the similar mode previously described in the Traena Basin (Figure 12). Such crustal removal could be largely controlled by a detachment faulting system observed along the western flank of the Nyk High and possibly on the eastern flank of the Grimm High/Hel Terrace lying on the conjugate side of the expected Paleocene rift/thinning axis (Figures 4b, c). Together with the breakup-related magmatism this thinning event could have promoted a collapse of the Hel Graben and uplift of the Nyk High as proposed in the model of Gernigon et al. (2003). Depositional patterns and the rapid Paleocene subsidence rates may indicate that the main phase of thinning took place during the Paleocene rifting phase restricted to the Hel Graben, and possibly underneath the basalt in the central outer part of the Vøring Margin (e.g. the Fenris Graben). Poorer seismic imaging at greater depth in the area makes hard to estimate the amount of crustal thinning in the earlier rifting phases. The possible presence of pre-Cretaceous sediments at the Grimm and Nyk highs (Figures 4a, b) allows us to speculate that the pre-Cretaceous basin on top of the thinned crust could also co-exist within the Hel Graben, although appropriate sediments could be highly metamorphosed and delaminated at least during Late Cretaceous-Paleocene rifting and likely during earlier extensional phases.

Compared to the Hel Graben, the crustal blocks preserved on the flanks (e.g. the Grimm High and Nyk High) show evidence of thicker continental crust (Figure 4b), less affected by the Paleocene thinning compared to the adjacent Hel Graben. We interpret this specific crustal configuration in terms of boudinage of the crust (Figure 12) (see Gartrell,

1997) which appears to be a key process in many other rifted margins worldwide (Clerc et al., 2017). The Nyk and Grimm highs most likely represent thick crustal swell or boudin in between the sub-basin (Hel Graben) where drastic thinning deformations were localized (Figure 12).

It is also important to note that the Hel Graben experienced a different tectonic history compared to the other segments of the outer Vøring Basin. Increasing faulting events and drastic Paleocene sedimentation in the Hel Graben (Figure 11f) are synchronous to uplift and progressive decrease of the normal faulting observed further south in the central segment of the outer Vøring Basin (e.g. North and South Gjallar ridges). We propose that this difference is possibly linked with the localization and migration of the deformation during the Paleocene. The crustal thinning estimation suggests that, in Paleocene, the Hel Graben was almost close to the breakup stage if we assume a crustal thickness of less than 4 km (Figure 4b, c). However, the breakup finally occurred 65 km further west. It suggests that the Paleocene rift axis that almost dissected the Hel Graben failed to propagate further south and jumped west of the Grimm High during the earliest Eocene breakup. The final jump is possibly explained by the onset of magmatism (Figure 12), likely leading to extra weakening and rift localization in the western branch of this complex overlapping system. Similar processes of rift migration/abortion triggered by magmatism and underplating are described in Yamasaki and Gernigon (2010).

5.3. Regional and generic implications

Early (Neocomian) and mid-Cretaceous extension in its regional context

We may identify evidence for significant Cretaceous tectonic activity in the northern Vøring Margin. While Late Jurassic-Early Cretaceous and Late Cretaceous-Paleocene extensional phases are widely accepted and confirmed by structural observations and drilling, Neocomian and mid-Cretaceous (Aptian to nearly Campanian) rifting events are often neglected, rather ambiguous and often interpreted as a passive sedimentary infill during post-rift thermal subsidence (Skogseid et al., 2000; Færseth and Lien, 2002; Færseth, 2012). Recent drilling results from the Vøring Basin, e.g. well 6603/5-1 at the South Gjallar Ridge and well 6608/2-1S at the Utgard High (NPD factpages, 2017) proved much thicker Lower and Upper Cretaceous sediments than previously believed (Blystad et al., 1995; Swecicki et al., 1998; Skogseid et al., 2000). Such misinterpretation in the proposed stratigraphy is primarily the results of previous underestimation of the sedimentation rates throughout the Cretaceous period and consequently may explain the minimization of the mid-Cretaceous extension (Faerseth & Lien, 2002). However, previous evidence for prominent early-to mid-Cretaceous extensional tectonism have been reported in the Rån and Gjallar Ridges in the outer Vøring Basin (Gernigon et al., 2003), the Lofoten-Vesterålen Margin (Tsikalas et al., 2001, 2005; Henstra et al., 2016), the Någrind Syncline and the Træna Basin (Figures 7, 12; this study). Aptian-Cenomanian extension at the southern end of the Nordland Ridge was also suggested by Pascoe et al. (1999). It is not impossible that this extensional deformation may have propagated north, along the flank of the Nordland Ridge, triggering mid-Cenomanian-Santonian extensional reactivation in the Træna Basin. Activation of the Nordland Ridge as a sand source in the Cenomanian and Turonian-Coniacian (Lysing Formation) was also

suggested by Doré et al. (1999) and Fjellanger et al. (2005). Furthermore, coeval tectonic reactivation was observed along the onshore continuation of the Møre-Trøndelag Fault Complex (Sømme et al., 2013). Nearly coeval apatite fission track ages (since 100 Ma) of fault reactivation and block uplift of kilometers scale within the Møre-Trøndelag Fault Complex have been reported from the Norwegian mainland (Redfield et al., 2005). Beyond that, in the wider North Atlantic realm, we have well-documented evidence of Early to mid-Cretaceous extension, including Aptian rifting in the SW Barents Sea (Faleide et al., 1993; Serck et al., 2017), mid-Albian faulting activity in the NE Greenland (Whitham et al., 1999) and Berriasian to Cenomanian syn-rift deposition in the Rockall Trough (Corfield et al., 1999). The prominent Late Mesozoic rifting phases in the Faeroe-Shetland Basin likely occurred in the Neocomian, Aptio-Albian, Cenomanian-Santonian and Campanian-Maastrichtian (Dean et al., 1999), whereas minor Turonian-Coniacian fault reactivation in the region promoted coeval sand deposition identical to Lysing Formation in the Norwegian Sea (Grant et al., 1999). All above mentioned structural observations make it likely that the entire mid-Norwegian Margin and the northern Vøring Margin segment, in particular, were subjected to similar early to mid-Cretaceous events in the regional context contrary to the quiescence interpretation of Færseth and Lien (2002). These events were possibly not associated with a prominent and continuous rifting axis in the mid-Norwegian Margin, but represented scattered, isolated and migrating rifting centers that were selectively reactivated along basement highs and old mobile zones (Lofoten Ridge, Nordland Ridge, Nyk High, Surt Lineament, Jan Mayen Corridor etc.).

On the role of crustal inheritance in the margin development and the presence of serpentinized mantle in the Vøring Basin

As mentioned above, recent tectonic models suggested a presence of a partially to heavily serpentinized mantle in the Vøring Basin (Reynisson et al., 2010; Rüpke et al., 2013; Peron-Pinvidic et al., 2013; Peron-Pinvidic and Osmundsen, 2016). Extremely thinned crust in the Hel Graben and the Træna Basin (Figure 4b) could favor such tectonic scenario there. Pérez-Gussinyé and Reston (2001) suggested that serpentinization can be likely achieved in the settings with thinning (beta) factors above 3 and a crustal thickness less than 8 km. However, in addition we have to consider the timing and duration of the main thinning phases, decompacted sediment thicknesses during these phases, and the development of basin-scale faults in order to understand environments that could promote or block water passage to the mantle and lead to a partial serpentinization. All these parameters should be then estimated, integrated and tested within different modelling approaches to allow testing of various hypotheses. However, our tectonic model also supports the early presence of inherited continental crust and related LCB over most of the highs observed in the Vøring Basin (Figure 12). It is unlikely that a broad zone of exhumed mantle affected the entire Vøring Basin, and the presence of exhumed mantle underneath the basalt cannot explain the shallow environments suggested by new seismic interpretation and petrology derived from the ODP drilling in the Vøring Marginal High (Abdelmalak et al., 2016a, 2016b). If serpentinization occurs, it would eventually be restricted to local windows in the deepest part of the sub-sag basin involved in this boudined and mullioned type of super-extension (Figure 12). Other observation from worldwide rifted margin (Clerc et al., 2017) but also various numerical models also support the presence and persistence of inherited crust underneath similarly large sag basins (Brune et al., 2014; Petersen and Schiffer, 2016).

The presence of older crustal grains and crustal weakness zones have a significant influence on basin development and architecture. While analogue and numerical models deal mostly with homogenous and uniform mode of extension in the rifted margins (Lavier and Manatschal, 2006), crustal inheritance and late magmatism could explain complex geometries and deformation migration and localization discussed in this paper. The inherited crustal blocks and associated structures/fabrics initiate and control the onset and development of thinning deformations of the continental crust (Abdelmalak et al., 2017). This "boudinage style of deformation" is similar to what has been previously described and proposed by Lister et al. (1986), Gartrell (1997) or Clerc et al. (2017). For the Northern Vøring and Lofoten-Vesterålen Margins, such a tectonic scenario was proposed almost 30 years ago by Anderson (1986) who, based on gravity anomalies analysis, suggested the existence of large scale boudinage of the continental crust which make up the margin. Furthermore, these weakness zones could be associated with major lithosphere structural discontinuities (e.g. sutures, mega-shear zones). Their orientation and deformational pattern could give us better constraints in paleorecontructions and better understand their role in the margin segmentation. Similar tectonic regimes occurred in the development of other rifted margins (Chian et al., 2001; Funck et al., 2008; Sun et al., 2009; Franke et al., 2014; Gernigon et al., 2014; Clerc et al., 2017). Therefore, we caution researchers to apply "classical" hyperextended Iberian scenarios in complex tectonic settings such as the mid-Norwegian margin. In the mid-Norwegian margin larger and thicker continental crustal masses with rather complex petrophysical properties and spatial distribution are involved. Its rift development is also polyphase and shows a much longer period of episodic rifting event compared to the Iberian rifted margin types.

6. CONCLUSIONS

1. We investigated and interpreted new seismic data in the northern Vøring Margin poorly constrained by deep seismic data in the past. Combined with regional map production and potential field modelling, we propose a new tectonic scenario for the mid-Norwegian margin.
2. We argue that the northern Vøring Margin and the entire mid-Norwegian margin were tectonically active during mid-Cretaceous in contrast to Færseth and Lien (2002). We found seismic evidence of Barremian-Aptian (?) faulting activity in the Någrind Syncline and mid-Cenomanian-Santonian extensional reactivation in the Træna Basin. This may indicate a non-uniform and non-linear distribution of rifting centers in the Early to mid-Cretaceous within the Vøring Margin likely reflecting selective tectonic reactivations along pre-existing mobile zones.
3. The Træna Basin is a narrow basin with a thin crust (4-5 km) which initiated since Late Jurassic as a half-graben developed on the flanks of the Utgard High. Possible later mid-Cenomanian-Santonian extensional reactivation significantly increased the basin subsidence and the thinning of the underlying continental crust. Pre-syn-rift and partly syn-rift sediments together with upper-mid crustal rocks at the basin floor might have been significantly deformed and delaminated/compacted during these extensional phases
4. According to our observations and modelling results the crust underneath the Utgard High likely represents ultra-high-density body (3200 kg/m^3) of Caledonian or older (Precambrian) origin. The top of this body corresponds to the strong *UH*-Reflection Detachment faults developed on the flanks of this rigid continental block and controlled the pre- and syn-thinning Mesozoic evolution of the adjacent basins (e.g. the Någrind Syncline and the Træna Basin).

5. We see no prerequisites to explain the configuration of the Någrind Syncline as a result of compressional buckling as previously suggested by Lundin et al. (2013). Our analysis shows that the Någrind Syncline has been formed by a migrating sequence of extensional and post-extensional events and associated vertical movements from the Early Cretaceous to final breakup in the earliest Eocene.
6. The Hel Graben is a deep Cretaceous-Paleocene basin that developed in between two rigid block ("continental buffers"). The thinning deformation in the Hel Graben was controlled by detachments on the flanks of these blocks (the Grimm High and the Nyk High) with a culmination in the Paleocene that led to a collapse of the structure. We suggest very thin upper and middle crustal rocks and pre- and syn-rift sediments in the axial part of the Hel Graben. They are most likely highly deformed and metamorphosed along detachments. Extremely thinned crust (3-4 km) indicates that the Hel Graben was very close to the breakup stage in the Paleocene until the rifting axes eventually jumped in the Late Paleocene-Earliest Eocene towards the present continent-ocean 'boundary'. We also found evidence of intra-Paleocene intrusive magmatism preceding the main magmatic event during the earliest Eocene continental breakup.
7. The *T*-Reflection observed underneath the North Gjallar Ridge extends towards the Grimm High and might be of the same origin, i.e. old inherited Caledonian lower crust. These structures could be part of a common structural trend before the Late Cretaceous-Paleocene extensional phase.
8. We do not expect wide zones of mantle exhumation and serpentinization in the Vøring Basin, however local areas of serpentinization could eventually develop in deep sub-basins with significantly thinned crust (Træna Basin and Hel Graben). Nonetheless, in our opinion, the mid-Norwegian margin represents a unique type of a volcanic rifted margin, where large inherited crustal blocks define a long and polyphase development

and a complex deformation distribution. Combined with the presence of SDRs along the continent-ocean transition, it has very little in common with the Iberian non-volcanic rifted margin types.

Appendix 1. Stratigraphic comment on well 6608/2-1S, Utgard High.

This appendix provides a detailed stratigraphic comment on the selected Cretaceous intervals and log pattern interpretation of well 6608/2-1S. The well 6608/2-1S has been analyzed by RPS Ichron. The raw results of biostratigraphic analyses and wireline logs have been provided by the Norwegian Petroleum Directorate (NPD) via the Diskos National Data Repository. After review and integration, these data formed the basis of stratigraphic interpretation.

Early Cretaceous interval

The Early Cretaceous interval is dated in both the main hole and ST2 bypass where the sidewall core samples have been analyzed providing stronger age confidence (Figure A1).

The top of the Langebarn Formation is defined with the use of the change in the log pattern and is supported with the presence of *Caudammina ovula crassa* foraminifera (Figure A1). The Albian interval of the formation is characterized with the sparse palynological assemblage, consistent with the interpretation, with rare presence of *Batioladinium micropodum*, *Muderongia asymmetrica* and taxa of a broad Early Cretaceous range. The presence of *Aptea polymorpha* is considered to be characteristic of the Albian period in the northern latitudes (Nøhr-Hansen, 1993).

The Late Aptian section of the well is characterized by the prominent gamma log pattern (Figure A1), suggesting the palaeoenvironments with the decreased level of oxygen typical for this age. The presence of *Cerbia tabulata, Aptea eisenacki* and increase in *A. polymorpha* confirm the dating for the interval (Costa and Davey, 1992). The presence of *Vesperopsis mayi* is typical for the northern latitudes (Nøhr-Hansen, 1993) and tentatively suggest stressed environment (Harding and Allen, 1995).

The Early Aptian is confirmed with the presence of the red stained foraminifera and LAD of *Ctenidodinium elegantulum, Sirmiodinium grossii* and *Pseudoceratium pelliferum* (Costa and Davey, 1992). The pronounce spike increase in gamma (Figure A1), together with abundant influx of bisaccate pollen grains and sapropelic organic in core, confirm the presence of OAE1 sediments, representing Selli event (Ainsworth et al., 2000). This interval is an equivalent to Fischschiefer bed in North Sea. The presence of *Subtilisphaera perlucida* is additional evidence of anoxic environment and confirms the age interpretation.

The presence of Barremian sediments within the section is supported with the downward change of the log pattern (Figure A1) and is confirmed with the LAD of *Aptea anaphrissa* and *Nelchinopsis kostromiensis*, together with the base of abundant presence of *P. cretaceum* and overall assemblage change (Costa and Davey, 1992).

Coniacian-Albian interval

The Lysing Formation, typically representing Turonian-Late Coniacian strata, is not prominently expressed in the log profile and has not been analyzed for biostratigraphy (Figure A1). The underlying interval is characterized by the rich assemblage indicative of Turonian age, present in two samples (Figure A1). The co-occurrence of acme event of *Palaeohystrichophora infusorioides* together with abundance of *Cauveridinium*

membraniphorum is indicative of latest Turonian (Olde et al., 2014; Costa and Davey, 1992). The co-occurring *Stephodinium coronatum* and *Apteodinium maculatum* serve as important markers as their LAD are observed at top Turonian boundary (Costa and Davey, 1992); specifically for North Træna and Møre basins (Radmacher et al., 2015; Smelror et al., 1994). The co-occurring *Heterosphaeridium difficile* is known to have its FAD within the Turonian (Costa and Davey, 1992); specifically in the North Træna Basin (*Radmacher et al*., 2015). The influx of *Surculosphaeridium longifurcatum*, observed in the sample below, is known to be characteristic of mid-Turonian strata (Costa and Davey, 1992; Radmacher et al., 2015).

Due to its lower thickness in comparison to the known sections of the basin, the Turonian interval of the well is considered to be either condensed or possessing a stratigraphic unconformity. Since the studied assemblages possess strong Middle-Late Turonian marker events and lack any Early Turonian events, this negative evidence is tentatively suggesting the presence of unconformity with the Early and partly Middle Turonian intervals missing from the section.

The underlying part of the Blålange Formation is characterized by extensively expanded section with its age defined in two samples from the upper part of the studied interval (Figure A1). The assemblage in these samples is represented by the abundant presence of *Subtilisphaera kalaatii* and other peredinoid cysts such as *Palaeoperidnium cretaceum* and *Palaeohystrichophora infusorioides*, together with increase of common *Chlamydophorella nyei* and single occurrences of *Rhombodella paucispina* and *Ovoidinium scabrosum*. These events suggest the correlation to the Palaeohystrichophora infusorioides – Paaeohystrichophora palaeoinfusa Interval Zone *sensu* Radmacher et al. (2014), and are indicative of Middle-Late Cenomanian.

The presence of the assemblages dominated with peridininoid cysts, specifically *Palaeoperidinium cretaceum* and *Subtilisphaera kalaatii*, in Cenomanian strata is characteristic for North Træna Basin (Radmacher et al., 2015), southwestern Barents Sea (Radmacher et al., 2014) and East Greenland (Nøhr-Hansen, 1993; 2012).

Appendix 2. A comment on the petrophysical properties used in the 2D potential field modelling of the northern Vøring transect.

All potential field studies combine *a priori* constraints such as physical property data, geological mapping or seismic interpretations to limit the infinite number of possible theoretical solutions (Saltus and Blakely, 2011). Some of the modelling assumptions derived mostly (1) from local onshore-offshore correlations of some gravity and magnetic anomalies; (2) the nature of the rocks expected; (3) the correlation with Vp values from refraction/OBS data; and (4) the conclusion of the potential field modelling itself.

Rock property data from onshore (see NGU database, e.g. Olesen et al., 2010) and local offshore density logs also provide local constrains, but mostly limited to the upper part of the sedimentary basin and/or the proximal part of the margin. We assume that the density in the deepest part of the basin does not exceed an average value of 2750 kg/m^3 which also fit conventional Vp/density function. This threshold value was also voluntarily chosen to reach the maximum of crustal thinning we could expect along the transect.

Sedimentary rocks are also almost non-magnetic (e.g. Olesen et al., 2010) and we assumed, accordingly, that most of the magnetic sources source from the crystalline basement or the basalt in the outer part of the margin.

Review of the onshore measurements (see Olesen et al., 2010) shows a large variation of the rock properties. However, all rocks from the upper part of the crust (e.g. the Caledonian nappes) have, in average, lower density and lower magnetic susceptibilities (<0.01-0.02 SI) compared to the pre-Cambrian crust showing higher density and much higher susceptibilities (>0.03 SI). Previous modellings have shown that a simple crustal model with an upper crust dominated by rocks equivalent of the Caledonian nappes and a magnetic middle crust associated with pre-Cambrian types of rocks could easily explain the observed gravity and magnetic signature of the Mid-Norwegian margin (e.g. Ebbing et al., 2006; Reynisson et al., 2010; Olesen et al., 2010; Gernigon et al., 2015; Maystrenko et al., 2017). The lower to the upper crust with Vp velocities higher than 7 km/s are most likely characterized by high density material as confirmed by our modelling (e.g. the prominent gravity anomaly of the Utgard High). In general, the crustal densities are also realistic and remain in the range of average crustal values measured at specific depth on the Earth (Herzberg et al., 1983; Christiensen and Mooney, 1995).

In addition to the forward modelling, we also consider Werner independent deconvolution techniques to estimate the potential field sources directly from measured anomalies without appeal to specific assumptions about the source distributions. When finally combined with seismic data, the final potential field model fits all observations and geophysical data available (e.g. seismic, gravity, magnetic). Therefore, if a model produces results that agree with data, we will regard it as successful until new data and understanding allow us to modify or even reject modelling results. The parameters in Table 1 just show the best parameters required to fit all the data and observations. Without extra constrain, a sensitivity analysis will only result in a minor variation of the relative crustal properties involved.

Acknowledgments

Funding for this work came from OMNIS Project: Offshore Mid-Norwegian: Integrated Margin and Basin Studies, (Project Number: 210429/E30) funded by the Norwegian Research Council through its Centre of Excellence CEED (Centre for Earth Evolution and Dynamics). The seismic, magnetic, and gravity data presented in this study were provided by TGS. RPS Ichron is acknowledged for performing biostratigraphic analysis of well 6608/2-1S. Seismic interpretation was done using IHS Kingdom software. Grid interpolations and map compilations were established using Geosoft Oasis Montaj and ArcGIS softwares. We would like to acknowledge First Geo AS and TGS for the use of hiQbe™ regional velocity cube employed in depth conversion. We thank GeoModelling Solutions for providing an academic license for TecMod 2D software. The seismic and well data used in this study are available through the Diskos National Data Repository (NDR). Well formation tops are also available at the NPD factpages (www.npd.no) and the NORLEX team website (www.nhm2.uio.no/norlex/). We are grateful to Jolante van Wijk (New Mexico Tech), Daniel Schmid (PGP, University of Oslo) and Sergei Medvedev (CEED, University of Oslo) for their help and fruitful discussions that improved the paper, and we thank Ben Manton (VBPR) for the linguistic remarks. We also would like to thank Christopher Jackson, Philip Ball and the Editor Nathan Niemi for their constructive and helpful reviews.

REFERENCES

Abdelmalak, M. M., T. B. Andersen, S. Planke, J. I. Faleide, F. Corfu, C. Tegner, G. E. Shephard, D. Zastrozhnov, and R. Myklebust (2015), The ocean-continent transition in the mid-Norwegian margin: Insight from seismic data and an onshore Caledonian field analogue, *Geology*, 43, 1011-1014, doi:10.1130/G37086.1.

Abdelmalak, M.M., R. Meyer, S. Planke, J.I. Faleide, L. Gernigon, Frieling, J., A. Sluijs, G-J. Reichart, D. Zastrozhnov, S. Theissen-Krah, A. Said, R. Myklebust, R. (2016a), Pre-breakup magmatism on the Vøring Margin: Insight from new sub-basalt imaging and results from Ocean Drilling Program Hole 642E, *Tectonophysics*, 675, 258-274, doi:10.1016/j.tecto.2016.02.037.

Abdelmalak, M. M., S. Planke, J. I. Faleide, D. A. Jerram, D. Zastrozhnov, S. Eide, and R. Myklebust (2016b), The development of volcanic sequences at rifted margins: New insights from the structure and morphology of the Vøring Escarpment, mid-Norwegian Margin, *J. Geophys. Res. Solid Earth*, 121, 5212–5236, doi: 10.1002/2015JB012788.

Abdelmalak M.M., J. I. Faleide, S. Planke, L. Gernigon, D. Zastrozhnov, G.E. Shephard and R. Myklebust (2017), The T-Reflection and the deep crustal structure of the Vøring Margin offshore Mid-Norway, *Tectonics, 36, 2497–2523*, https://doi.org/10.1002/2017TC004617.

Ainsworth, N.R., L.A. Riley, and L.T. Gallagher (2000), An Early Cretaceous lithostratigraphic and biostratigraphic framework for the Britannia Field reservoir (Late Barremian–Late Aptian), UK North Sea, *Petroleum Geoscience*, 6 (4), 345-367.

Allen, P. A., and J. R. Allen (2013), Basin Analysis: Principles and Application to Petroleum Play Assessment, pp. 642, John Wiley.

Anderson, J.A. (1986), Arctic geodynamics: the opening of the Arctic Ocean, *Adv. Space Res*., 6, 9, 79—63, doi: 10.1016/0273-1177(86)90356-X.

Bergh, S.G., Eig, K, Kløvjan, O.S., Henningsen, T., Olesen, O. & Hansen, J.A. (2007), The Lofoten-Vesterålen continental margin: a multiphase Mesozoic-Palaeogene rifted shelf as shown by offshore-onshore brittle fault-fracture analysis, *Norwegian Journal of Geology*, 87, 29-58.

Berndt, C., O. P. Skogly, S. Planke, O. Eldholm, and R. Mjelde (2000), High-velocity breakup-related sills in the Vøring Basin, off Norway, *Journal of Geophysical Research*, 105, 28, 443-428, 454.

Blystad, P., H. Brekke, R. B. Færseth, B. T. Larsen, J. Skogseid, and B. Tørudbakken (1995), Structural elements of the Norwegian continental shelf Part II: the Norwegian Sea Region, *NPD-Bulletin*, The Norwegian Petroleum Directorate, 8.

Bjørnseth, H. M., S. M. Grant, E. K. Hansen, J. R. Hossack, D. G. Roberts, and M. Thompson (1997), Structural evolution of the Vøring Basin, Norway, during the Late Cretaceous and Paleogene, *Journal of the Geological Society (London)*, v. 154, no. 3, p. 559–563, doi:10.1144/gsjgs.154.3.0559.

Brekke, H. & Riis, F (1987), Tectonics and basin evolution of the Norwegian shelf between 62°N and 72°N, *Norsk Geologisk Tidsskrift*, 67, pp. 295-322.

Brekke, H., S. Dahlgren, B. Nyland & C. Magnus (1999), The prospectivity of the Vøring and Møre Basins on the Norwegian Sea continental margin, *Geological Society, London, Petroleum Geology Conference series*, 5, 261–274, doi: 10.1144/0050261.

Brekke, H. (2000), The tectonic evolution of the Norwegian Sea Continental Margin with emphasis on the Vøring and Møre Basins, *Geological Society, London, Special Publications*, 167(1), 327-378, doi:10.1144/gsl.sp.2000.167.01.13.

Brune, S.; A.A. Popov, S.V. Sobolev (2012), Modeling suggests that oblique extension facilitates rifting and continental break-up, *Journal of Geophysical Research*, 117, B08402. doi:10.1029/2011JB008860.

Brune, S., C. Heine, M. Perez-Gussinye, S.V. Sobolev (2014), Rift migration explains continental margin asymmetry and crustal hyper-extension, *Nature Communications*, 5, doi:10.1038/ncomms5014.

Brune, S., S. E. Williams, N. P. Butterworth, and R. D. Müller (2016), Abrupt plate accelerations shape rifted continental margins, *Nature*, doi:10.1038/nature18319.

Buck, W. R. (2006), The role of magma in the development of the Afro-Arabian rift system, in *The Afar Volcanic Province within the East African Rift System*, edited by Yirgu, G., C.J. Ebinger and P.K.H. Maguire, *Geological Society, London, Special Publications*, 259, 43–54.

Chian, D., I. D. Reid, and H. R. Jackson (2001), Crustal structure beneath Orphan Basin and implications for nonvolcanic continental rifting, *J. Geophys. Res.*, 106(B6), 10,923–10,940, doi:10.1029/2000JB900422.

Christensen, N. I. and W.D. Mooney (1995), Seismic velocity structure and composition of the continental crust: a global view, *Journal of Geophysical Research: Solid Earth*, 100(B6), 9761-9788, doi: 10.1029/95JB00259.

Christie-Blick, N. and K.T. Biddle (1985), Deformation and basin formation along strike-slip faults, *SEPM Special Publication*, 37, 1–34, doi:10.2110/pec.85.37.0001.

Clark, S. A., E. Glørstad-Clark, J.I. Faleide, D. Schmid, E.H. Hartz, and W. Fjeldskaar, (2014), Southwest Barents Sea rift basin evolution: comparing results from backstripping and time-forward modelling, *Basin Research*, 26, 550-566, doi:10.1111/bre.12039

Clerc, C., A. Lahfid, P. Monié, Y. Lagabrielle, C. Chopin, M. Poujol, P. Boulvais, J.-C. Ringenbach, E. Masini, M. de St Blanquat (2015), High-temperature metamorphism during extreme thinning of the continental crust: a reappraisal of the north Pyrenean paleo-passive margin, *Solid Earth*, 6, 643–668, doi:10.5194/se-6-643-2015.

Clerc, C., Y. Lagabrielle, P. Labaume, J-C. Ringenbach, A. Vauchez, T. Nalpas, R. Bousquet, J-F. Ballard, A. Lahfid, S. Fourcade (2016). Basement – Cover decoupling and progressive exhumation of metamorphic sediments at hot rifted margin. Insights from the Northeastern Pyrenean analog, *Tectonophysics*, 686, 82-97, doi:10.1016/j.tecto.2016.07.022.

Clerc, C., Ringenbach, J.-C., Jolivet, L., Ballard, J.-F. (2017), Rifted margins: Ductile deformation, boudinage, continentward-dipping normal faults and the role of the weak lower crust, *Gondwana Research*, doi:10.1016/j.gr.2017.04.030.

Cohen, K.M., S.C. Finney, P.L. Gibbard and J.-X. Fan (2013), The ICS International Chronostratigraphic Chart, *Episodes*, 36, 3, 199-204.

Corfield, S., N. Murphy and S. Parker (1999), The structural and stratigraphic framework of the Irish Rockall Trough, *Geological Society, London, Petroleum Geology Conference series*, 5, 407-420, doi:10.1144/0050407.

Costa, L.I. & R.J. Davey (1992), Dinoflagellate Cysts of the Cretaceous System, In: Powell, A.J. (Ed), A Stratigraphic Index of Dinoflagellate Cysts, Chapman & Hall, London.

Dalland, A., D. Worsley and K Ofstad (1988), A lithostratigraphic scheme for the Mesozoic and Cenozoic succession offshore mid- and northern Norway, *NPD Bulletin 4*, 63 p.

Dean, K., K. McLachlan and A. Chambers (1999), Rifting and the development of the Faeroe–Shetland Basin, *Geological Society, London, Petroleum Geology Conference series*, 5, 533–544, doi:10.1144/0050533.

Digranes, P., R. Mjelde, S. Kodaira, H. Shimamura, T. Kanazawa, H. Shiobara, E.W. Berg (1998), A regional shear-wave velocity model in the central Vøring Basin, N. Norway, using three-component ocean bottom seismographs, *Tectonophysics*, 293, 157– 174, doi:10.1016/S0040-1951(98)00093-6.

Doré, A. G., E. R. Lundin, L. N. Jensen, Ø. Birklamd, P. E. Eliassen, and C. Fichler (1999), Principal tectonic events in the evolution of the northwest European Atlantic margin, *Geological Society, London, Petroleum Geology Conference series*, 5, 41-61, doi:10.1144/0050041.

Doré, A.G., E.R. Lundin, N.J. Kusznir and C. Pascal (2008), Potential mechanisms for the genesis of Cenozoic domal structures on the NE Atlantic margin: Pros and cons and some new ideas, in *The Nature and Origin of Compression in Passive Margins. Geological Society, London, Special Publications*, 306, edited by H. Johnson, A.G. Doré, R.W. Gatliff, R. Holdsworth, E.R. Lundin and J.D. Ritchie, 1–26, doi:10.1144/SP306.1.

Ebbing, J., E. Lundin, O. Olesen, and E. K. Hansen (2006), The mid-Norwegian margin: a discussion of crustal lineaments, mafic intrusions, and remnants of the Caledonian root by 3D density modelling and structural interpretation, *Journal of the Geological Society*, London, 163, 47-59, doi:10.1144/0016-764905-029.

Ebinger, C., and M. Casey (2001), Continental breakup in magmatic provinces: An Ethiopian example, *Geology*, 29, 527–530, doi:10.1130/0091-7613(2001)029<0527:CBIMPA>2.0.CO;2.

Eldholm, O., J. Thiede, and E. Taylor (1989), Evolution of the Vøring Volcanic Margin, in *Proceedings of the Ocean Drilling Program, Scientific Results*, edited by O. Eldholm, J. Thiede, and E. Taylor, pp. 1033–1065, Ocean Drilling Program, College Station, Tex.

Eldholm, O., F. Tsikalas, and J. I. Faleide (2002), Continental margin off Norway 62–75°N: Palaeogene tectono-magmatic segmentation and sedimentation, *Geol. Soc. London Spec. Publ.*, 197(1), 39–68, doi:10.1144/gsl.sp.2002.197.01.03.

Faleide, J.I., E. Vågnes and S.T. Gudlaugsson (1993), Late Mesozoic-Cenozoic evolution of the southwestern Barents Sea in a regional rift-shear tectonic setting, *Marine and Petroleum Geology*, 10, 186–214, doi:10.1016/0264-8172(93)90104-Z.

Faleide, J. I., F. Tsikalas, A. J. Breivik, R. Mjelde, O. Ritzmann, Ø. Engen, J. Wilson, and O. Eldholm (2008), Structure and evolution of the continental margin off Norway and the Barents Sea, *Episodes*, 31(No. 1), 82-91.

Fjellanger, E., F. Surlyk, L.C. Wamsteeker and T. Midtun (2005), Upper Cretaceous basin-floor fans in the Vøring Basin, Mid Norway shelf, in *Onshore-Offshore Relationships on the North Atlantic Margin, Norwegian Petroleum Society Special Publications*, 12, edited by B. Wandås, J.P. Nystuen, E. Eide and F.M. Gradstein, 135–164, doi:10.1016/S0928-8937(05)80047-5.

Foulger, G.R. (2010), Plates vs Plumes: A Geological Controversy, Wiley-Blackwell, Oxford.

Franke, D. (2013), Rifting, lithosphere breakup and volcanism: Comparison of magma-poor and volcanic rifted margins, *Marine and Petroleum Geology*, 43, p. 63–87, doi:10.1016/j.marpetgeo.2012.11.003.

Franke, D., D. Savva, M. Pubellier, S. Steuer, B. Mouly, J. L. Auzietre, F. Meresse, and N. Chamot-Rooke (2014), The final rifting evolution in the South China Sea, *Mar. Pet. Geol.*, 1–17, doi:10.1016/j.marpetgeo.2013.11.020.

Funck, T., M. S. Andersen, J. K. Neish, and T. Dahl-Jensen (2008), A refraction seismic transect from the Faroe Islands to the Hatton-Rockall Basin, *J. Geophys. Res.*, 113, B12405, doi:10.1029/2008JB005675.

Færseth, R.B. and T. Lien (2002), Cretaceous evolution in the Norwegian Sea – a period characterized by tectonic quiescence, *Marine and Petroleum Geology*,19, 1005–1027, doi:10.1016/S0264-8172(02)00112-5.

Færseth, R.B. (2012), Structural development of the continental shelf offshore Lofoten–Vesterålen, northern Norway, *Norwegian Journal of Geology*, 92, 19-40.

Gartrell, A. P. (1997), Evolution of rift basins and low-angle detachments in multilayer analog models, *Geology*, 25(7), 615–618, doi:10.1130/0091-7613(1997)025<0615:EORBAL>2.3.CO;2.

Geoffroy, L., E.B. Burov, P. Werner (2015), Volcanic passive margins: another way to break up continents, *Sci. Rep.*, 5, doi: 10.1038/srep14828

Gernigon, L., J.-C. Ringenbach, S. Planke, and H. Jonquet-Kolsto (2003), Extension, crustal structure and magmatism at the outer Vøring Basin, Norwegian margin, *Journal of Geological Society*, London, 160, 197-208, doi:10.1144/0016-764902-055.

Gernigon, L., J.-C. Ringenbach, S. Planke, and B. Le Gall (2004), Deep structures and breakup along volcanic rifted margins: insights from integrated studies along the outer Vøring Basin (Norway), *Marine and Petroleum Geology*, 21(3), 363-372, doi:10.1016/j.marpetgeo.2004.01.005.

Gernigon, L., M. Brönner, D. Roberts, O. Olesen, A. Nasuti, and T. Yamasaki (2014), Crustal and basin evolution of the southwestern Barents Sea: From Caledonian orogeny to continental breakup, *Tectonics*, 33, 347-373, doi:10.1002/2013TC003439.

Gernigon, L., A. Blischke, A. Nasuti, and M. Sand (2015), Conjugate volcanic rifted margins, seafloor spreading, and microcontinent: Insights from new high-resolution

aeromagnetic surveys in the Norway Basin, *Tectonics*, 34, 907–933, doi:10.1002/2014TC003717.

Gradstein, F.M., E. Anthonissen, H. Brunstad, M. Charnock, Ø. Hammer, T. Hellem, K.S. Lervik (2010), Norwegian Offshore Stratigraphic Lexicon (NORLEX), *Newsl.Stratigr*. 44, 73-86.

Grant, N., A. Bouma and A. Mcintyre (1999), The Turonian play in the Faeroe-Shetland Basin, *Geological Society, London, Petroleum Geology Conference series*, 5,661-673, doi:10.1144/0050661.

Gomez, M., J. Verges, M. Fernandez, M. Torne, C. Ayala, W. Wheeler, R. Karpuz (2004), Extensional geometry of the Mid Norwegian Margin before Early Tertiary continental breakup, *Marine and Petroleum Geology*, 21, 177–194, https://doi.org/10.1016/j.marpetgeo.2003.11.017.

Harding, I., R Allen (1995), Dinocysts and the palaeoenvironmental interpretation of non-marine sediments: an example from the Wealden of the Isle of Wight (Lower Cretaceous, southern England), *Cretaceous Research*, 16, 727 – 743.

Harry D. L., J.C. Bowling (1999), Inhibiting magmatism on nonvolcanic rifted margins, *Geology*, 27, 895–898, https://doi.org/10.1130/0091-7613(1999)027<0895:IMONRM>2.3.CO;2.

Henstra, G.A., R.L. Gawthorpe, W. Helland-Hansen, R. Ravnås and A. Rotevatn (2016), Depositional systems in multiphase rifts: seismic case study from the Lofoten margin, Norway, *Basin Research*, 1–23, doi:10.1111/bre.12183.

Herzberg, C. T., W. S. Fyfe, and M. J. Carr (1983), Density constraints on the formation of the continental Moho and crust, *Contributions to Mineralogy and Petrology*, 84(1), 1-5, doi: 10.1007/BF01132324.

Hjelstuen, B.O., O. Eldholm and J. Skogseid (1999), Cenozoic evolution of the northern Vøring Margin, *Geological Society of America Bulletin* 111, 1792–1807, doi: 10.1130/0016-7606(1999)111<1792:CEOTNV>2.3.CO;2.

Huismans, R.S. and C. Beaumont (2011), Depth-dependent extension, two-stage breakup and cratonic underplating at rifted margins, *Nature*, 473, http://dx.doi.org/10.1038/nature09988.

Imber, J., R.E. Holdsworth, K.J.W. McCaffrey, R.W. Wilson, R.R. Jones, R.W. England and G. Gjeldvik (2005), Early Tertiary sinistral transpression and fault reactivation in the western Vøring Basin, Norwegian Sea: implications for hydrocarbon exploration and

pre-breakup deformation in ocean margin basins, *AAPG bulletin*. 89 (8), 1043-1069, doi:10.1306/02240504043.

Kittelsen, J. E., R.R. Olsen, R.F. Marten, E.K. Hansen and R.R. Hollingsworth (1999), The first deepwater well in Norway and its implications for the Upper Cretaceous Play, Vøring Basin, *Geological Society, London, Petroleum Geology Conference series*, 5, 275-280, doi: 10.1144/0050275.

Kjennerud, T. and L. Vergara (2005), Cretaceous to Palaeogene 3D palaeobathymetry and sedimentation in the Vøring Basin, Norwegian Sea, in *Petroleum Geology: North-West Europe and Global Perspectives—Proceedings of the 6th Petroleum Geology Conference*, edited by A.G. Doré and B.A. Vining, 815–831.

Kusznir, N.J., R. Hunsdale, A.M. Roberts, iSIMM Team (2005), Timing and magnitude of depth-dependent lithosphere stretching on the S. Lofoten and N. Vøring continental margins offshore mid-Norway: implications for subsidence and hydrocarbon maturation at volcanic rifted margins, in *Petroleum Geology: North-West Europe and Global Perspectives—Proceedings of the 6th Petroleum Geology Conference*, edited by A.G. Doré and B.A. Vining, 767–783,

Lavier, L. L., and G. Manatschal (2006), A mechanism to thin the continental lithosphere at magma-poor margins, *Nature*, 440 (7082), 324–328, doi:10.1038/nature04608.

Lister, G. S., M. A. Etheridge, and P. A. Symonds (1986), Detachment faulting and the evolution of passive continental margins, *Geology*, 14, 246–250, doi:10.1130/0091-7613(1986)14<246:DFATEO>2.0.CO;2.

Lundin, E. R. and A.G. Doré (1997), A tectonic model for the Norwegian passive margin with implications for the NE Atlantic: early Cretaceous to break-up, *Geological Society London Journal*, 154, 545–550, doi: 10.1144/gsjgs.154.3.0545.

Lundin, E.R., K. Rønning, A.G. Doré and O. Olesen (2002), Hel Graben, Vøring Basin, Norway - a possible major cauldron?, paper presented at 25th Nordic Geological Winter Meeting, 6–9 January, Reykjavik, Abstract Volume, 132.

Lundin, E.R and A.G. Doré (2011), Hyperextension, serpentinization, and weakening: A new paradigm for rifted margin compressional deformation, *Geology*, 39, 347-350, doi: 10.1130/G31499.1.

Lundin, E.R., A.G. Doré, K. Rønning and R. Kyrkjebø (2013), Repeated inversion and collapse in the Late Cretaceous-Cenozoic northern Vøring Basin, offshore Norway, *Petroleum Geoscience*, 19, 329-341, doi:10.1144/petgeo2012-022.

Maystrenko, Y. P., O. Olesen, L. Gernigon, and S. Gradmann (2017), Deep structure of the Lofoten-Vesterålen segment of the Mid-Norwegian continental margin and adjacent areas derived from 3-D density modeling, *J. Geophys. Res. Solid Earth*, 122, doi:10.1002/2016JB013443.

McKenzie, D. (1978), Some remarks on the development of sedimentary basins, *Earth and Planetary Science Letters*, 40, 25–32, doi:10.1016/0012-821X(78)90071-7.

Meyer, R., J. van Wijk and L. Gernigon (2007), The North Atlantic Igneous Province: a review of models for its formation, in *Plates, Plumes and Planetary processes, Geological Society of America Special Paper*, 430 edited by G.R. Foulger and D.M. Jurdy, 525-552, doi:10.1130/2007.2430(26).

Mjelde, R., S. Kodaira, H. Shimamura, T. Kanazawa, H. Shiobara, E.W. Berg, O. Riise (1997), Crustal structure of the central part of the Vøring Basin, mid-Norway margin, from ocean bottom seismographs, *Tectonophysics* 277, 235-257, doi:1016/S0040-1951(97)00028-0.

Mjelde, R., P. Digranes, H. Shimamura, H. Shiobara, S. Kodaira, S., H. Brekke, T. Egebjerg, N. Sørenes, T. Thorbjørnsen (1998), Crustal structure of the northern part of the Vøring Basin, mid-Norway margin, from wide-angle seismic and gravity data, *Tectonophysics* 293, 175–205, doi:10.1016/S0040-1951(98)00090-0.

Mjelde, R., T. Raum, P. Digranes, H. Shimamura, H. Shiobara, S. Kodaira (2003), Vp/Vs ratio along the Vøring Margin, NE Atlantic, derived from OBS data: implications on lithology and stress field, *Tectonophysics* 369, 175-197, doi:10.1016/S0040-1951(03)00198-7.

Mjelde, R., A. Goncharov, and R. D. Müller (2013), The Moho: Boundary above upper mantle peridotites or lower crustal eclogites? A global review and new interpretations for passive margins, *Tectonophysics*, 609, 636-650, doi:10.1016/j.tecto.2012.03.001.

Mjelde, R., T. Kvarven, J.I. Faleide, H. Thybo (2016), Lower crustal high-velocity bodies along North Atlantic passive margins, and their link to Caledonian suture zone eclogites and Early Cenozoic magmatism, *Tectonophysics*, 670, 16-29, doi: 10.1016/j.tecto.2015.11.021.

Mogensen, T. E., R. Nyby, R. Karpuz, and P. Haremo (2000), Late Cretaceous and Tertiary structural evolution of the northeastern part of the Vøring Basin, Norwegian Sea, in *Dynamics of the Norwegian margin: Geological Society (London) Special Publication*, 167, edited by A. Nøttvedt et al., 379–396, doi: 10.1144/GSL.SP.2000.167.01.14.

Morton, A. C. and S. Grant (1998), Cretaceous depositional systems in the Norwegian Sea: Heavy mineral constraints, *AAPG Bulletin*, 82(2), 274-290.

Mosar, J. (2000), Depth of extensional faulting on the Mid-Norway Atlantic passive margin, *Norgesqeoloqiske undersekelse Bulletin* 437, 33-41.

Mosar, J., E.A. Eide, P.T. Osmundsen, A. Sommaruga and T. Torsvik (2002), Greenland-Norway separation: A geodynamic model for the North Atlantic, *Norwegian Journal of Geology*, 82, 281–298.

Neumann, E.-R., H. Svensen, C. Tegner, S. Planke, M. Thirlwall, K.E. Jarvis (2013), Sill and lava geochemistry of the mid-Norway and NE Greenland conjugate margins, *Geochemistry, Geophysics, Geosystems*, 14, 3666-3690, doi: 10.1002/ggge.20224.

Nirrengarten, M., L. Gernigon, G. Manatschal (2014), Lower crustal bodies in the Møre volcanic rifted margin: Geophysical determination and geological implications, *Tectonophysics*, 636, 143-157, doi:10.1016/j.tecto.2014.08.004.

Ní Dheasúna, M., M. Ballesteros, J. Leven (2012), A regional velocity cube for depth conversion on the Northwest Shelf, *PESA News Resources*, August/September, 2012, 40-43, available online at: www.pnronline.com.au/article.aspx?p=1&id=810

Norwegian Petroleum Directorate (NPD) (2017), Factpages, available at: http://factpages.npd.no/factpages/ (last access: April 2017).

Nøhr-Hansen, H. (1993), Dinoflagellate cyst stratigraphy of the Barremian to Albian, Lower Cretaceous, North-East Greenland, *Bull. Grønl. Geol. Unders*., 166, 1–171.

Nøhr-Hansen, H. (2012), Palynostratigraphy of the Cretaceous–lower Palaeogene sedimentary succession in the Kangerlussuaq Basin, southern East Greenland, *Rev. Palaeobot. Palynol.*, 178, 59–90.

Olde, K., I. Jarvis, M. M. Pearce, D. Uličný, B. Tocher, J. Trabucho-Alexandre, D. Gröcke, (2014), A revised northern European Turonian (Upper Cretaceous) dinoflagellate cyst biostratigraphy: Integrating palynology and carbon isotope events, *Rev. Palaeobot. Palynol.*, 213, 1-16.

Olesen O., M. Brönner, J.Ebbing. J. Gellein, L. Gernigon, J.Koziel, T. Lauritsen, R. Myklebust, C. Pascal, M. Sand, D. Solheim and S. Usov (2010), New aeromagnetic and gravity compilations from Norway and adjacent areas - Methods and applications, in *Petroleum Geology: From Mature Basins to New Frontiers, Proceedings of the 7th Petroleum Geology Conference*, edited by B. A. Vining and S. C. Pickering, 559–586, Geol. Soc., London.

Osmundsen, P.T. and J. Ebbing (2008), Style of extension offshore mid-Norway and implications for mechanisms of crustal thinning at passive margins, *Tectonics*, 27, 1-12, doi: 10.1029/2007TC002242.

Osmundsen, P.T., A. Sommaruga, J.R. Skilbrei, O. Olesen (2002), Deep structure of the Mid-Norway rifted margin. *Nor. J. Geol*. 82, 205–224.

Osmundsen, P.T., Péron-Pinvidic, G., Ebbing, J., Erratt, D., Fjellanger, E., Bergslien, D. & Syvertsen, S.E. (2016), Extension, hyperextension and mantle exhumation offshore Norway: a discussion based on 6 crustal transects, *Norwegian Journal of Geology*, 96, 343–372, doi: 10.17850/njg96-4-05.

Pascoe, R., R. Hooper, K. Storhaug and H. Harper (1999), Evolution of extensional styles at the southern termination of the Nordland Ridge, Mid-Norway: a response to variations in coupling above Triassic salt, *Geological Society, London, Petroleum Geology Conference series*, 5, 83–90, doi:10.1144/0050083.

Pérez-Gussinyé, M., T.J. Reston (2001), Rheological evolution during extension at nonvolcanic rifted margins: onset of serpentinization and development of detachments leading to continental breakup, *Journal of Geophysical Research: Solid Earth (1978–2012)* 106, 3961–3975, doi:10.1029/2000JB900325.

Péron-Pinvidic, G., G. Manatschal, and P. T. Osmundsen (2013), Structural comparison of archetypal Atlantic rifted margins: A review of observations and concepts, *Mar. Petrol. Geol.*, 43, 21–47, doi:10.1016/j.marpetgeo.2013.02.002.

Péron-Pinvidic, G. and P.T. Osmundsen (2016), Architecture of the distal and outer domains of the Mid-Norwegian rifted margin: Insights from the Rån-Gjallar ridges system, *Marine and Petroleum Geology*, 77, 280-299, doi:10.1016/j.marpetgeo.2016.06.014.

Péron-Pinvidic, G., P.T. Osmundsen and J. Ebbing (2016), Mismatch of geophysical datasets in distal rifted margin studies, *Terra Nova*, 28, 340–347. https://doi.org/10.1111/ter.12226.

Petersen, K. D., and C. Schiffer (2016), Wilson cycle passive margins: Control of orogenic inheritance on continental breakup, *Gondwana Research*, 39, 131-144, doi:10.1016/j.gr.2016.06.012.

Pinel, V., and C. Jaupart (2005), Caldera formation by magma withdrawal from a reservoir beneath a volcanic edifice, *Earth Planet. Sci. Lett*., 230, 273–287, doi:10.1016/j.epsl.2004.11.016.

Planke, S., J. Skogseid, O. Eldholm (1991), Crustal structure off Norway, 62–70^{0}N, *Tectonophysics*, 189, 91–107, doi:10.1016/0040-1951(91)90489-F.

Radmacher, W., J. Tyszka, G. Mangerud, M.A. Pearce (2014), Dinoflagellate cyst biostratigraphy of the Late Albian to Early Maastrichtian in the southwestern Barents Sea, *Mar. Pet. Geol.*, 57, 109–121.

Radmacher, W., G. Mangerud, J. Tyszka (2015), Dinoflagellate cyst biostratigraphy of Upper Cretaceous strata from two wells in the Norwegian Sea, *Rev. Palaeobot. Palynol.*, 216, 18-32.

Redfield, T.F., A. Braathen, R.H. Gabrielsen, P.T. Osmundsen, T. Torsvik and P.A.M. Andriessen (2005), Late Mesozoic to Early Cenozoic components of vertical separation across the Møre Trøndelag Fault Complex, Norway, *Tectonophysics*, 395, 233–249, doi:10.1016/j.tecto.2004.09.012.

Ren, S., J. Skogseid, and O. Eldholm (1998), Late Cretaceous–Paleocene extension on the Vøring volcanic margin, *Marine Geophysical Researches*, 20, 4, 343–369, doi:10.1023/A:1004554217069.

Ren, S., J.I. Faleide, O. Eldholm, J. Skogseid and F. Gradstein (2003), Late Cretaceous-Paleocene development of the NW Vøring Basin, *Marine and Petroleum Geology*, 20, 177–206, doi:10.1016/S0264-8172(03)00005-9.

Reynisson, R. F., J. Ebbing, E. Lundin, and P. T. Osmundsen (2010), Properties and distribution of lower crustal bodies on the mid-Norwegian margin, *Geological Society, London, Petroleum Geology Conference series*, 7, 843-854, doi:10.1144/0070843.

Rise, L., D. Ottesen, K. Berg, E. Lundin (2005), Large-scale development of the mid-Norwegian margin during the last 3 million years, *Marine and Petroleum Geology*, 22, 33–44, doi:10.1016/j.marpetgeo.2004.10.010.

Roberts, A.M., R.I. Corfield, N.J. Kusznir, S.J. Matthews, E.-K. Hansen and R.J. Hooper (2009), Mapping palaeostructure and palaeobathymetry along the Norwegian Atlantic continental margin, Møre and Vøring basins, *Petroleum Geoscience*, 15, 27-43, doi: 10.1144/1354-079309-804.

Rosenbaum, G., K. Regenauer-Lieb and R.F. Weinberg (2010), Interaction between mantle and crustal detachments: A nonlinear system controlling lithospheric extension, *J. Geophys. Res.*, 115 (B11412), doi:10.1029/2009JB006696.

Rüpke, L. H., S.M. Schmalholz, D.W. Schmid and Y.Y. Podladchikov (2008), Automated thermotectonostratigraphic basin reconstruction: Viking Graben case study, *AAPG Bulletin*, 92, 309-326, doi:10.1306/11140707009.

Rüpke, L. H., D.W. Schmid, E.H. Hartz and B. Martinsen (2010), Basin modelling of a transform margin setting: structural, thermal and hydrocarbon evolution of the Tano Basin, Ghana, *Petroleum Geoscience*, 16, 283-298, doi:10.1144/1354-079309-905.

Rüpke, L. H., D. W. Schmid, M. Perez-Gussinye, and E. Hartz (2013), Interrelation between rifting, faulting, sedimentation, and mantle serpentinization during continental margin formation-including examples from the Norwegian Sea, *Geochem. Geophys. Geosyst.*, 14, 4351–4369, doi:10.1002/ggge.20268.

Saltus, R.W. and R.J. Blakely (2011), Unique geologic insights from "non-unique" gravity and magnetic interpretation, *GSA Today*, 4-10, doi:10.1130/G136A.1.

Scheck-Wenderoth, M., T. Raum, J.I. Faleide, R. Mjelde, B. Horsfield (2007), The transition from the continent to the ocean: a deeper view on the Norwegian margin, *J. Geol. Soc. Lond.*, 164, 855–868, doi:10.1144/0016-76492006-131.

Scheck-Wenderoth, M. and Y. P. Maystrenko (2011), 3D lithospheric-scale structural model of the Norwegian continental margin (the Vøring and Møre basins), *Scientific Technical Report STR11/02 – Data*, GFZ Potsdam, doi:10.2312/GFZ.b103-11027.

Serck, C.S., J.I. Faleide, A. Braathen, B. Kjølhamar, A. Escalona, (2017), Jurassic to Early Cretaceous basin configuration (s) in the Fingerdjupet Subbasin, SW Barents Sea, *Marine and Petroleum Geology*, 86, 874-891, doi: 10.1016/j.marpetgeo.2017.06.044.

Simon, K., R.S. Huismans and C. Beaumont (2009), Dynamical modelling of lithospheric extension and small-scale convection: implications for magmatism during the formation of volcanic rifted margins, *Geophysical Journal International*, 176, 327-350, doi:10.1111/j.1365-246X.2008.03891.x.

Skogseid, J., O. Eldholm and V.B. Larsen (1992), Vøring Basin: subsidence and tectonic evolution, in *Structural and Tectonic Modeling and its Application to Petroleum Geology. Norwegian Petroleum Society, Special Publications*, 1, edited by R.M. Larsen, H. Brekke, B.T. Larsen and E. Talleraas, 55-82.

Skogseid, J., S. Planke, J.I. Faleide, T. Pedersen, O. Eldholm, F. Neverdal (2000), NE Atlantic continental rifting and volcanic margin formation, in *Dynamics of the Norwegian margin: Geological Society (London) Special Publication,* 167, edited by A. Nøttvedt et al., 295-326, doi:10.1144/GSL.SP.2000.167.01.12.

Slagstad, T., Davidsen, B. & Daly, J.S. (2011), Age and composition of crystalline basement rocks on the Norwegian continental margin: offshore extension and continuity of the Caledonian–Appalachian orogenic belt, *Journal of the Geological Society, London*, 168, 1167-1185, doi: 10.1144/0016-76492010-136.

Smelror, M., T. Jacobsen, L. Rise, O. Skarbø, J.G. Verdenius & J.O. Vigran (1994), Jurassic to Cretaceous stratigraphy of shallow cores on the Møre Basin Margin, Mid-Norway, *Norsk Geologisk Tidsskrift*, 74, 89-107.

Sun, Z., D. Zhou, S. M. Wu, Z. H. Zhong, K. Myra, J. Q. Jiang, and H. Fan (2009), Patterns and dynamics of rifting on passive continental margin from shelf to slope of the northern South China Sea: Evidence from 3D analogue modeling, *J. Earth Sci. China*, 20(1), 136–146, doi:10.1007/s12583-009-0011-6.

Swiecicki, T., P.B. Gibbs, G.E. Farrow and M.P. Coward (1998), A tectonostratigraphic framework for the mid-Norway region, *Marine and Petroleum Geology*, 15, 3, 245–276, doi:10.1016/S0264-8172(97)00029-9.

Sømme, T.O. and C.A.L. Jackson (2013), Source-to-sink analysis of ancient sedimentary systems using a subsurface case study from the Møre–Trøndelag area of southern Norway: Part 2 – sediment dispersal and forcing mechanisms, *Basin Research*, 25, 512–531, doi: 10.1111/bre.12014.

Talwani, M. (1973), Computer usage in the computation of gravity anomalies, *Methods Comput. Phys*., 13, 343–389.

Talwani, M. and O. Eldholm (1977), Evolution of the Norwegian-Greenland Sea, *Bull. Geol. Soc. Am.*, 88, 969-999, doi:10.1130/0016-7606(1977)88<969:EOTNS>2.0.CO;2.

ten Brink, U.S., and Z. Ben-Avraham (1989), The anatomy of a pull-apart basin: Seismic reflection observations of the Dead Sea Basin, *Tectonics*, 8, 333-350, doi:10.1029/TC008i002p00333.

Theissen-Krah, S., and L. H. Rüpke (2010), Feedbacks of sedimentation on crustal heat flow: New insights from the Vøring Basin, Norwegian Sea, *Basin Research*, 22, 976–990, doi:10.1111/j.1365-2117.2009.00437.

Theissen-Krah, S., Zastrozhnov, D., Abdelmalak, M.M., Schmid, D.W., Faleide, J.I., Gernigon, L. (2017), Tectonic evolution and extension at the Møre Margin – Offshore mid-Norway, *Tectonophysics*, 721, 227-238, doi:10.1016/j.tecto.2017.09.009.

Thomsen, L. (1986), Weak elastic anisotropy, *Geophysics*, 51(10), 1954-1966, doi:10.1190/1.1442051.

Tsikalas, F., J.I. Faleide and O. Eldholm (2001), Lateral variations in tectono-magmatic style along the Lofoten-Vesterålen margin off Norway, *Marine and Petroleum Geology*, 18, 807–832, doi:10.1016/S0264-8172(01)00030-7.

Tsikalas, F., J.I. Faleide, O. Eldholm and J. Wilson (2005), Conjugate mid-Norway and NE Greenland continental margins, in *Petroleum Geology: North-West Europe and*

Global Perspectives—Proceedings of the 6th Petroleum Geology Conference, edited by A.G. Doré and B.A. Vining, 785–801.

Tsikalas, F., J.I. Faleide, N.J. Kuznir (2008), Along-strike variations in rifted margin crustal architecture and lithosphere thinning between northern Vøring and Lofoten margin segments off mid-Norway, *Tectonophysics*, 458, 68-81, doi:10.1016/j.tecto.2008.03.001.

Van Avendonk, H.J.A., L. L. Lavier, D.J. Shillington, and G. Manatschal (2009), Extension of continental crust at the margin of the eastern Grand Banks, Newfoundland, *Tectonophysics*, 468, 131-148, doi: 10.1016/j.tecto.2008.05.030.

van Wijk, J.W., R.S. Huismans, M. Ter Voorde and S.A.P.L. Cloetingh (2001), Melt generation at volcanic continental margins: no need for a mantle plume?, *Geophysical Research Letters*, 28, 3995-3998, doi: 10.1029/2000GL012848.

van Wijk, J., D. Koning, G. Axen, D. Coblentz, E, Gragg,B Sion, (2018), Tectonic subsidence, geoid analysis, and the Miocene-Pliocene unconformity in the Rio Grande rift, southwestern United States: Implications for mantle upwelling as a driving force for rift opening, *Geosphere*, doi: 10.1130/GES01522.1.

Vergara, L., I. Wreglesworth, M. Trayfoot and G. Richardsen (2001), The distribution of Cretaceous and Paleocene deep-water reservoirs in the Norwegian Sea basins, *Petroleum Geoscience*, 7, 395-408, doi:10.1144/petgeo.7.4.395.

Vågnes, E., R.H. Gabrielsen and P. Haremo (1998), Late Cretaceous-Cenozoic intraplate contractional deformation at the Norwegian continental shelf: timing, magnitude and regional implications, *Tectonophysics*, 300, 29–46, doi:10.1016/S0040-1951(98)00232-7.

Walker, I.M., K.A. Berry, J.R. Bruce, L. Bystøl, and J.H. Snow (1997), Structural modelling of regional depth profiles in the Vøring Basin: implications for the structural and stratigraphic development of the Norwegian passive margin, *Journal of the Geological Society, London*, 154, 537–544, doi:10.1144/gsjgs.154.3.0537.

Wangen, M., R. Mjelde, and J. I. Faleide (2011), The extension of the Vøring margin (NE Atlantic) in case of different degrees of magmatic underplating, *Basin Research*, 23(1), 83-100, doi:10.1111/j.1365-2117.2010.00467.x.

White, N.J. and D.P. McKenzie (1988), Formation of the "Steer's Head" geometry of sedimentary basins by differential stretching of the crust and mantle, *Geology*, 16, 250–253, doi:10.1130/0091-7613(1988)016<0250:FOTSSH>2.3.CO;2.

White, R.S. and D.P. McKenzie (1989), Magmatism at rift zones: The generation of volcanic continental margins and flood basalts, *Journal of Geophysical Research*, 94, 7685-7729, doi:10.1029/JB094iB06p07685.

White, R. S., L. K. Smith, A. W. Roberts, P. A. F. Christie, N. J. Kusznir, and & the rest of the iSIMM Team (2008), Lower-crustal intrusion on the North Atlantic continental margin, *Nature*, 452, 460-465, doi:10.1038/nature06687.

White, R. S., J. D. Eccles, and A. W. Roberts (2010), Constraints on volcanism, igneous intrusion and stretching on the Rockall–Faroe continental margin, *Petroleum Geology Conference series*, 7, 831-842, doi:10.1144/0070831.

Whitham, A. G., S.P. Price, A.M. Koriani and S.R.A. Kelly (1999), Cretaceous (post-Valanginian) sedimentation and rift events in NE Greenland (71-77°N), *Geological Society, London, Petroleum Geology Conference series*, 5, 325-336, doi: 10.1144/0050325.

Xie, X., and P.L. Heller (2009), Plate tectonics and basin subsidence history, *GSA Bulletin*, 121, 55–64, doi:10.1130/B26398.1.

Yamasaki, T and L. Gernigon (2009), Styles of lithospheric extension controlled by underplated mafic bodies, *Tectonophysics*, 468, 169-184, doi: 10.1016/j.tecto.2008.04.024.

Yamasaki, T., and L. Gernigon (2010), Redistribution of the lithosphere deformation by the emplacement of underplated mafic bodies: Implications for microcontinent formation, *J. Geol. Soc. London*, 167(5), 961–971, doi:10.1144/0016-76492010-027.

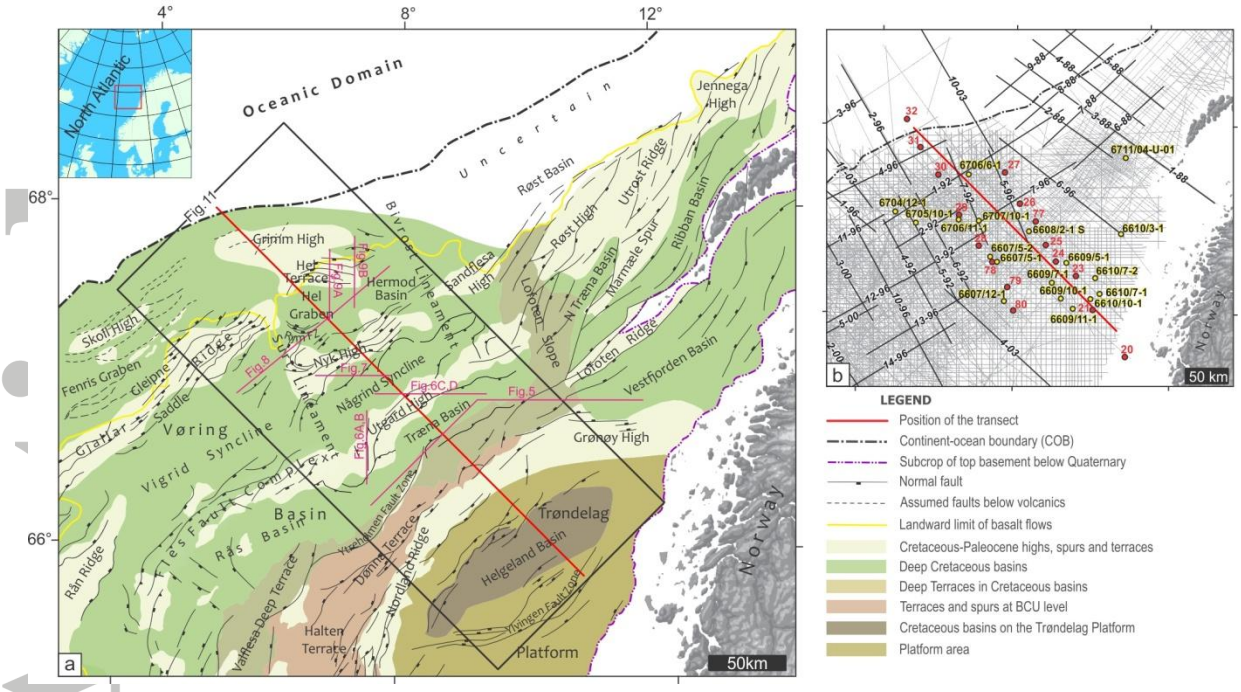

Figure 1. (a) Updated nomenclature map of the northern mid-Norwegian margin with pre-breakup structural elements. The fault pattern is mainly based on this study and modified from Blystad et al. (1995) and Gernigon et al. (2003). Locations of seismic close-ups are shown in purple solid lines. Extent of isochore maps is defined by black rectangle. (b) Geological and geophysical dataset used in this study: red circles – Expended Spread Profiles (centers), solid black lines – Ocean Bottom Seismometers profiles, solid light gray lines – reflection seismic, yellow circles – main wells used in this study.

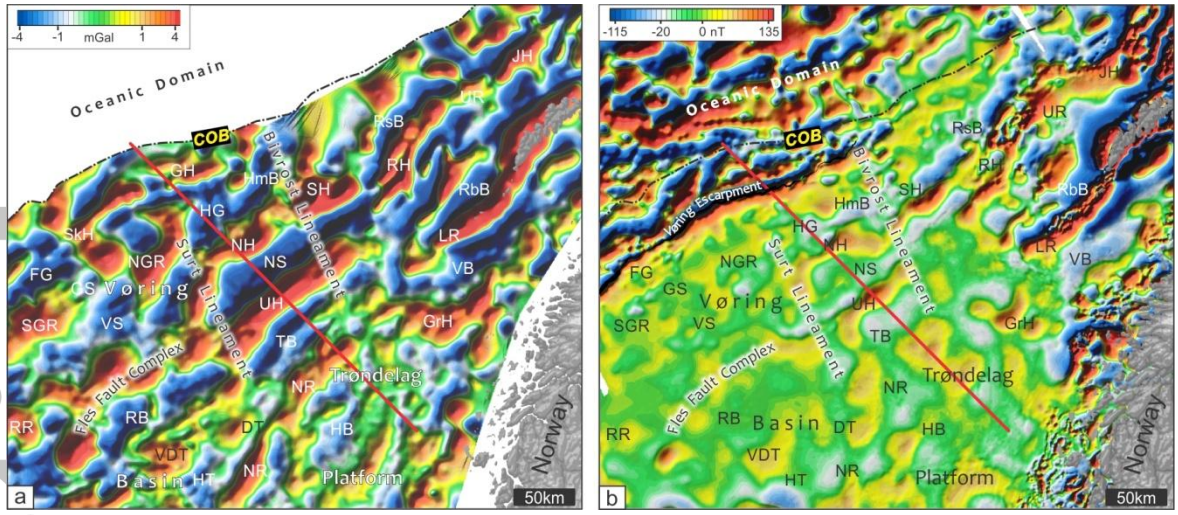

Figure 2. Potential field data for the northern Vøring Margin. (a) 50-km high-pass filtered Bouguer data. (b) 50-km high pass filtered magnetic data. DT – Donna Terrace, FG – Fenris Graben, GH – Grimm High, GS – Gleipne Saddle, GrH – Grønøy High, HB – Helgeland Basin, HG – Hel Graben, HT – Halten Terrace, HmB – Hermod Basin, LR – Lofoten Ridge, NGR – North Gjallar Ridge, NH – Nyk High, NS – Någrind Syncline, JH – Jennega High, RB – Rås Basin, RH – Røst High, RR – Rån Ridge, RbB – Ribban Basin, RsB – Røst Basin, SGR – South Gjallar Ridge, SH – Sandflesa High, SkH – Skoll High, TB – Træna Basin, UH – Utgard High, UR – Utrøst Ridge, VB – Vestfjorden Basin, VDT – Valflesa Deep Terrace, VS – Vigrid Syncline. Data by courtesy of TGS.

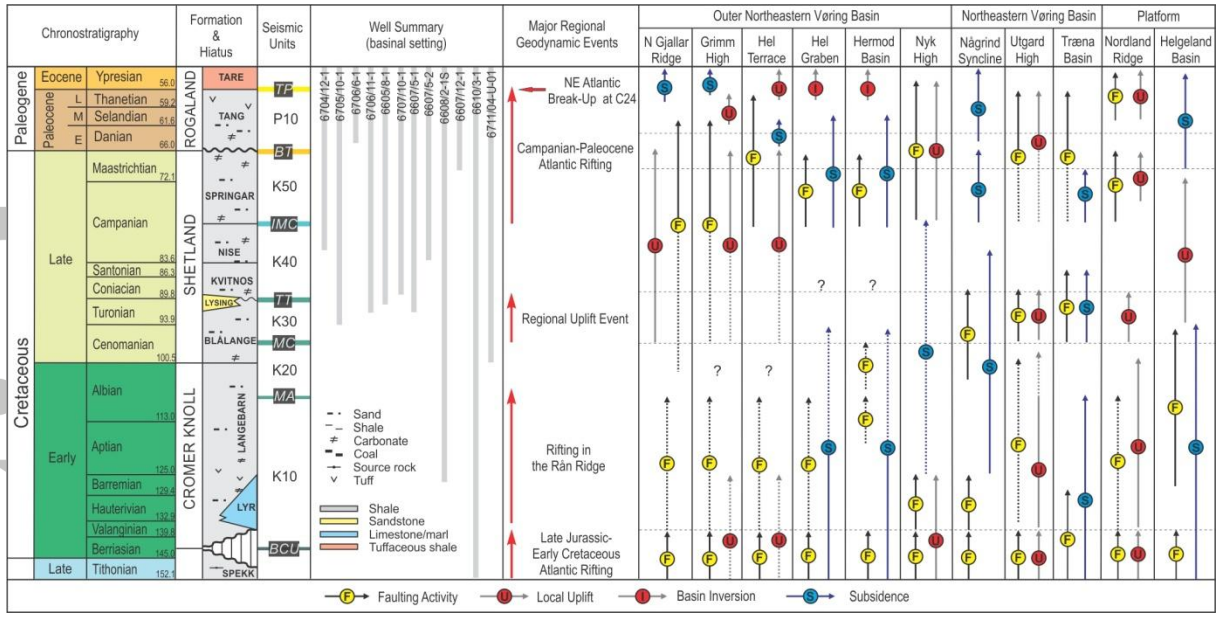

Figure 3. Tectonostratigraphic summary of the study area. Time scale after Cohen et al. (2013).

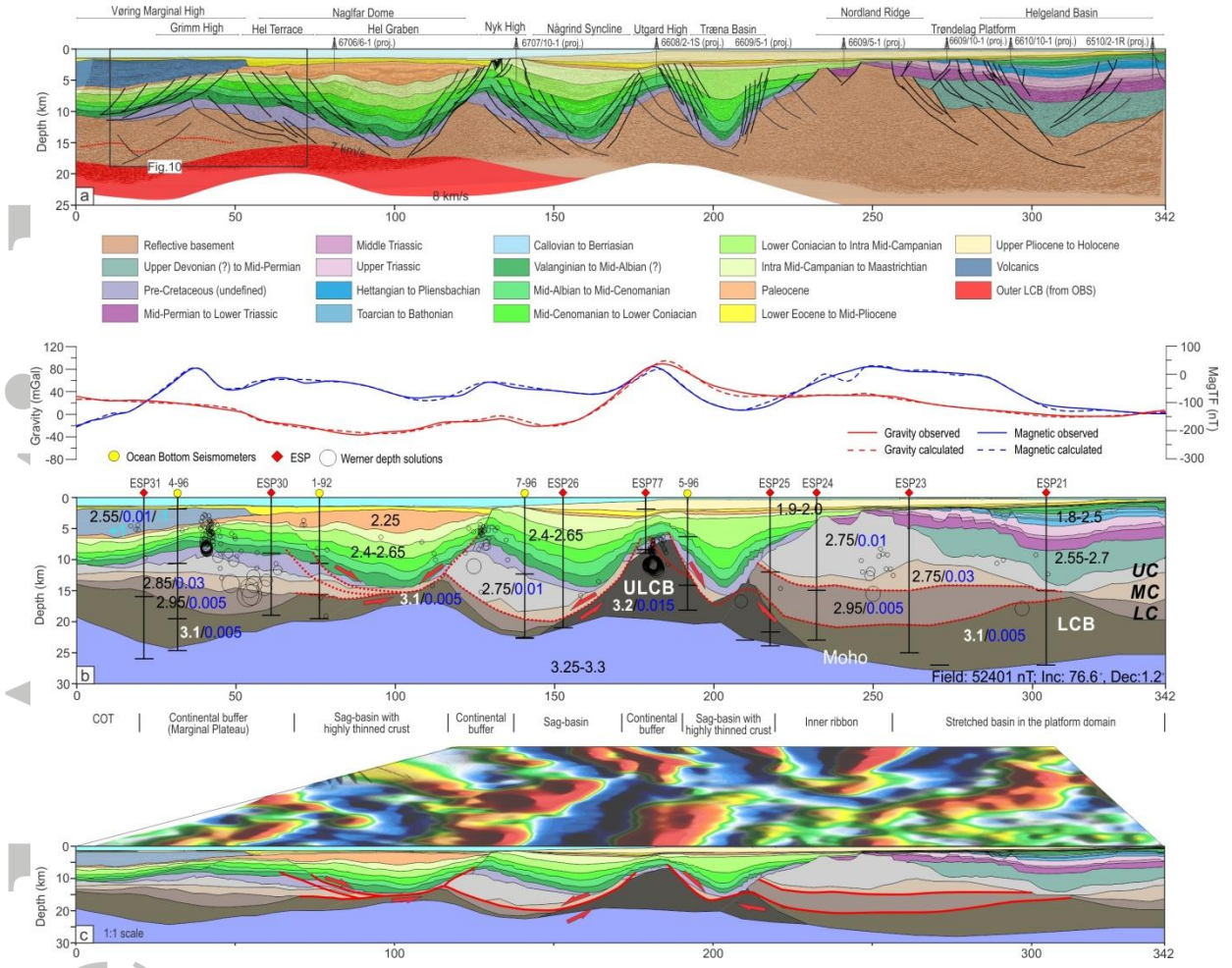

Figure 4. Crustal transect across the northern Vøring Margin derived from seismic observations (a) and potential field modelling (b) (see figure 1a for location). (c) Similar section at 1:1 scale with structural features discussed in the text. In the northern Vøring Margin we propose a model of crustal boudinage where sag basins with thin and very thin crust are separated by rigid continental 'buffers'. LC – lower crust, LCB – lower crustal body, MC – middle curst, UC – upper crust, ULCB – ultra-high density lower crustal body. Note differences between the interpreted and modeled transect in the central Hel Graben, where we have to remove pre-Cretaceous sediments in order to get better fit with the gravity.

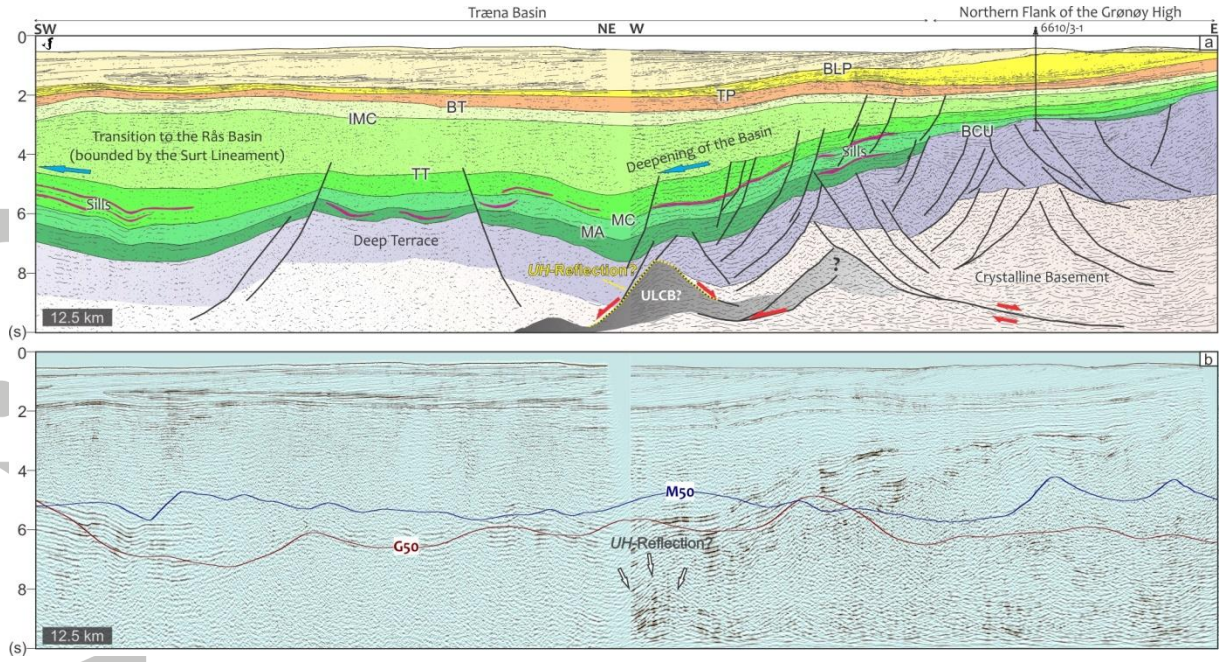

Figure 5. Composite seismic line showing configuration of the deep Træna Basin with relatively thin lower Cretaceous and thick upper Cretaceous successions: (a) interpreted and (b) uninterpreted. Pre-Cretaceous fault blocks are underlain by the deep crustal reflection associated with the increase of a gravity signal and could be related to a basin continuation of the ultra-high density lower crustal body (ULCB) observed in the Utgard High (see figs.4b and 6). G50 - 50-km high-pass filtered Bouguer anomaly pseudohorizon; M50 – 50-km high pass filtered magnetic data pseudo-horizons. The common legend for the sedimentary part is shown on figure 4. The abbreviations for the horizons are given in the text in the part 3.1. Location of the seismic line is shown on figure 1a. Data by courtesy of TGS

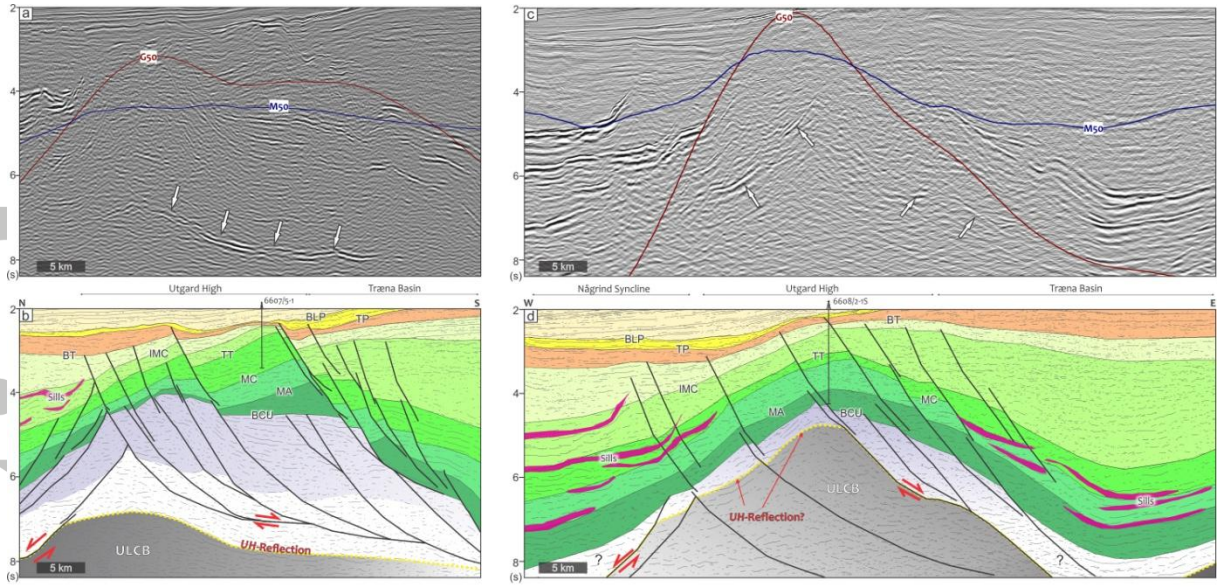

Figure 6. Structure of the Utgard High and configuration of the ULCB. Southern Segment: (a) uninterpreted and (b) interpreted seismic sections. Northern Segment: (c) uninterpreted and (d) interpreted seismic sections. White arrows on the uninterpreted sections point at the *UH*-Reflection interpreted as the top of the ULCB. Note significant increase of the gravity and magnetic signals (G50 and M50, respectively) in the northern segment of the high. The common legend for the sedimentary part is shown on figure 4. The abbreviations for the horizons are given in the text in the part 3.1. Location of the seismic line is shown on figure 1a. Data by courtesy of TGS.

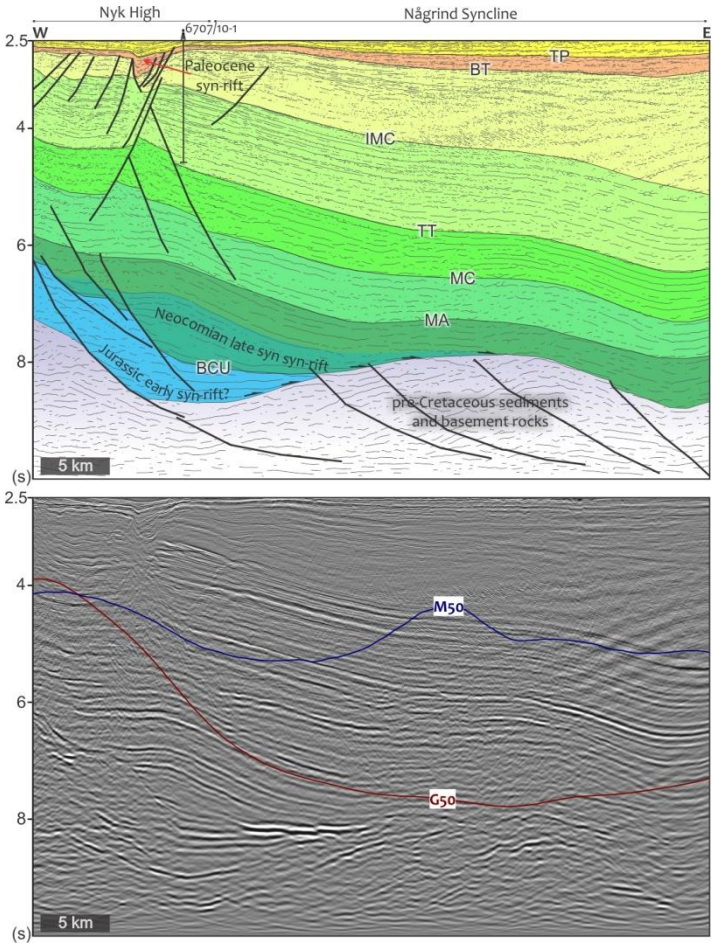

Figure 7. Seismic line across the Någrind-Nyk segment of the study area: (a) interpreted and (b) uninterpreted. Here we can recognize Jurassic and Neocomian syn-rift wedges developed on the eastern flank of the Nyk-High. The deep and old syn-rift sequences are controlled by an east-dipping faults. Maastrichtian-Paleocene rifting in the area was associated with west dipping faulting, the uplift of the Nyk High, and significant subsidence of the Någrind Syncline where a large depocentre was formed. The common legend for the sedimentary part is shown on figure 4. The abbreviations for the horizons are given in the text in the part 3.1. Location of the seismic line is shown on figure 1a. Data by courtesy of TGS.

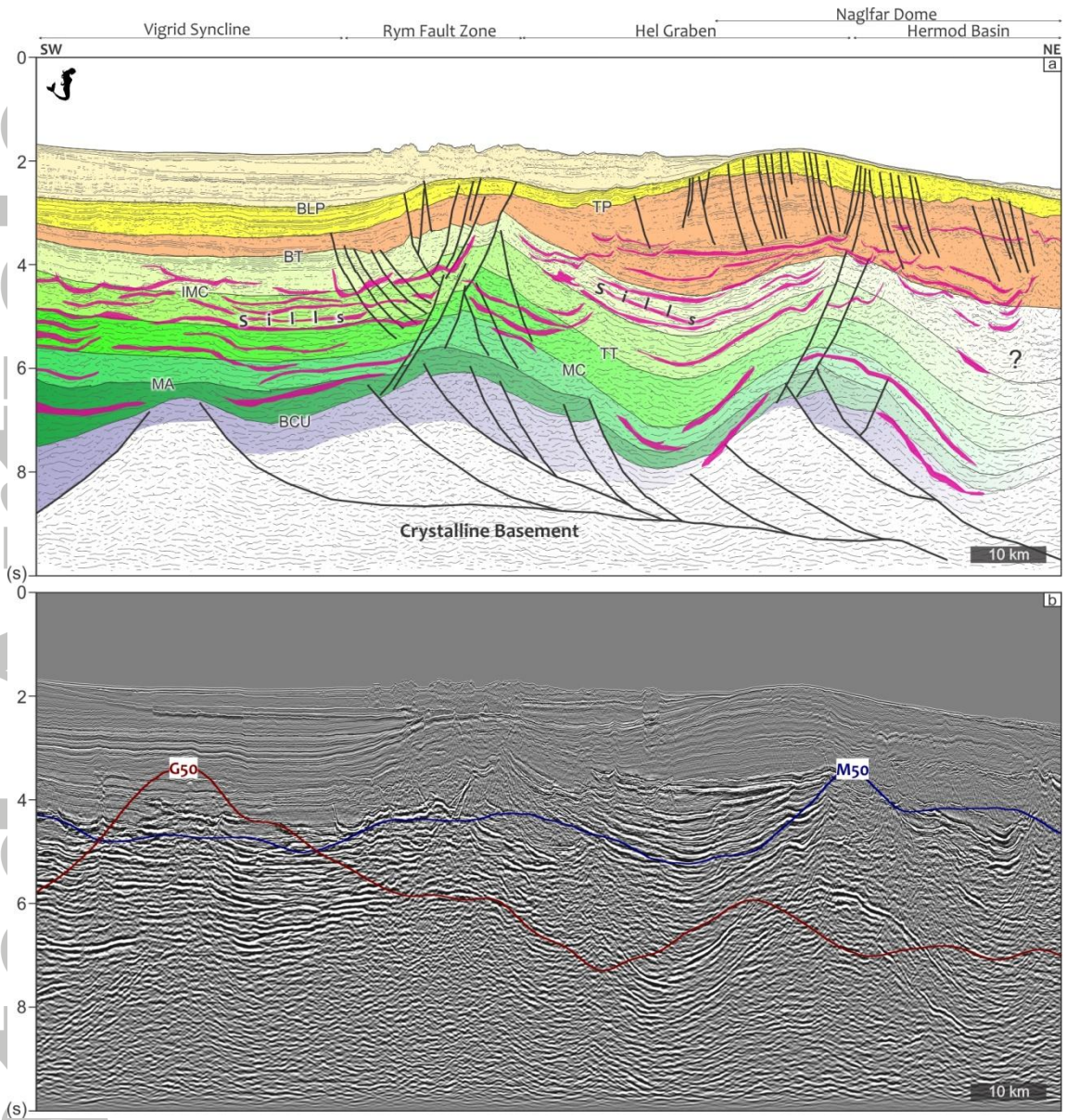

Figure 8. Seismic tie from the Vigrid Syncline to the Hel Graben revealing the deep configuration of the basin formed underneath thick Paleocene successions: (a) interpreted and (b) uninterpreted line. The Hel Graben and the adjacent Hermod Basin are structurally divided by a deep-seated structural high. The common legend for the sedimentary part is shown on figure 4. The abbreviations for the horizons are given in the text in the part 3.1. Location of the seismic line is shown on figure 1a. 50-km high-pass filtered Bouguer gravity (G50) and magnetic (M50) anomalies shown. Data by courtesy of TGS.

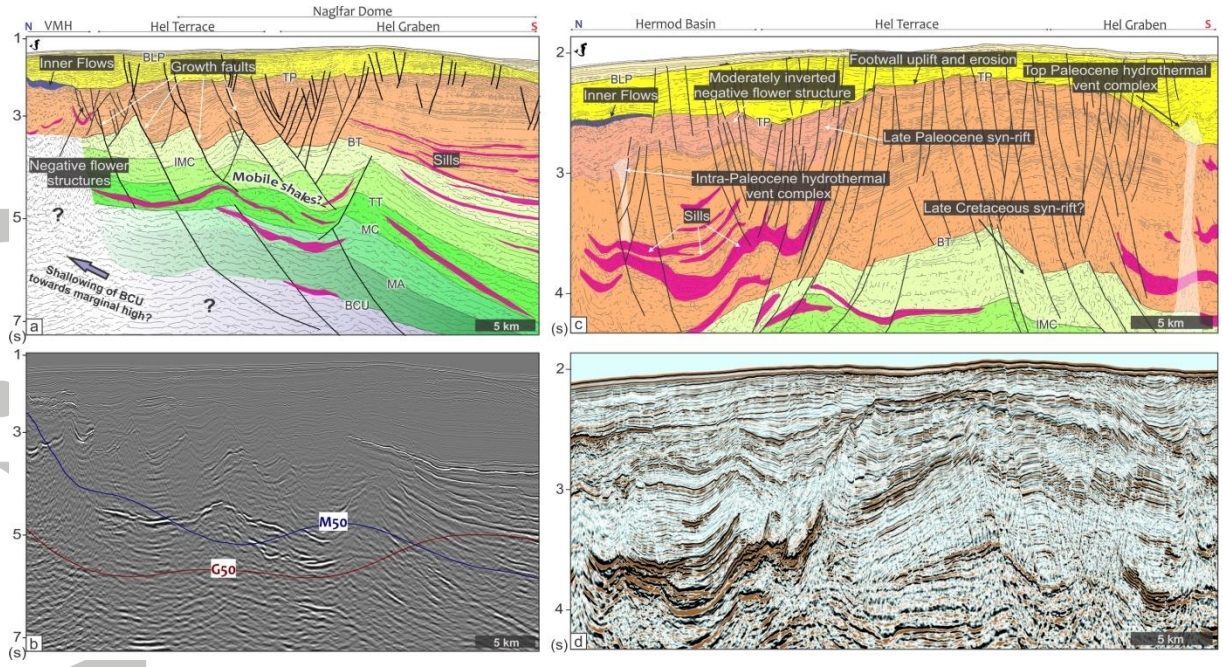

Figure 9. Seismic lines across the Hel Terrace and the Hel Graben. Lines (a) and (b) (interpreted and uninterpreted, respectively): central part of the Hel Terrace with Paleocene rift structures (growth faults) that are controlled at depth by probable lower-mid-Cretaceous mobile shales. Later in Paleocene the structure was mildly reactivated in strike-slip regime. Increase of the gravity signal towards the Vøring Marginal High could correspond to the shallowing of the BCU level and presence of pre-Cretaceous high/terrace below volcanics. Lines (c) and (d) (interpreted and uninterpreted, respectively): eastern part of the Hel Terrace. Late Cretaceous syn-rift sequences could develop in the central part of the structure and then superimposed by thick Paleocene sediments related to the collapse of the Hel Graben. Later in Paleocene the northern flank of the Hel Terrace was affected by rifting and associated rift-shoulder uplift and erosion. This event was preceded by minor sill intrusion expressed by a venting developed in Paleocene sequences. Major magmatic activity occurred at Paleocene-Eocene transition with extensive sill intrusions (shown in purple) and development of magmatic sequences at the Vøring Marginal High (Inner Flows). 50-km high-pass filtered Bouguer gravity (G50) and magnetic (M50) anomalies shown for the figure 7a only. The common legend for the sedimentary part is shown on figure 4. The abbreviations for the horizons are given in the text in the part 3.1. Location of the seismic lines is shown on figure 1a. Data by courtesy of TGS.

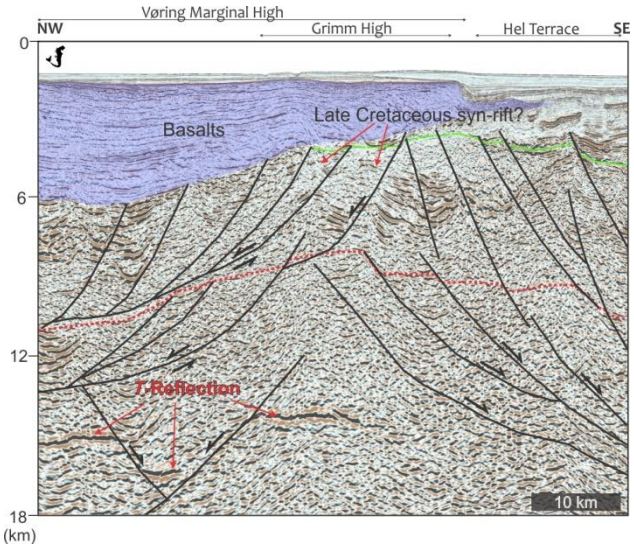

Figure 10. A part of the studied depth-converted transect (see figure 4a) adjacent to continent-ocean 'boundary' showing sub-basalt configuration of the Grimm High. Tilted fault-blocks below volcanics could develop within Cretaceous sequences on the analogue with the North Gjallar Ridge (see Gernigon et al., 2003). At about 15 km deep and faulted crustal reflection (*T*-Reflection) is observed. Base Tertiary and Base Cretaceous Unconformities are shown in dashed green and dotter red, respectively. Data by courtesy of TGS.

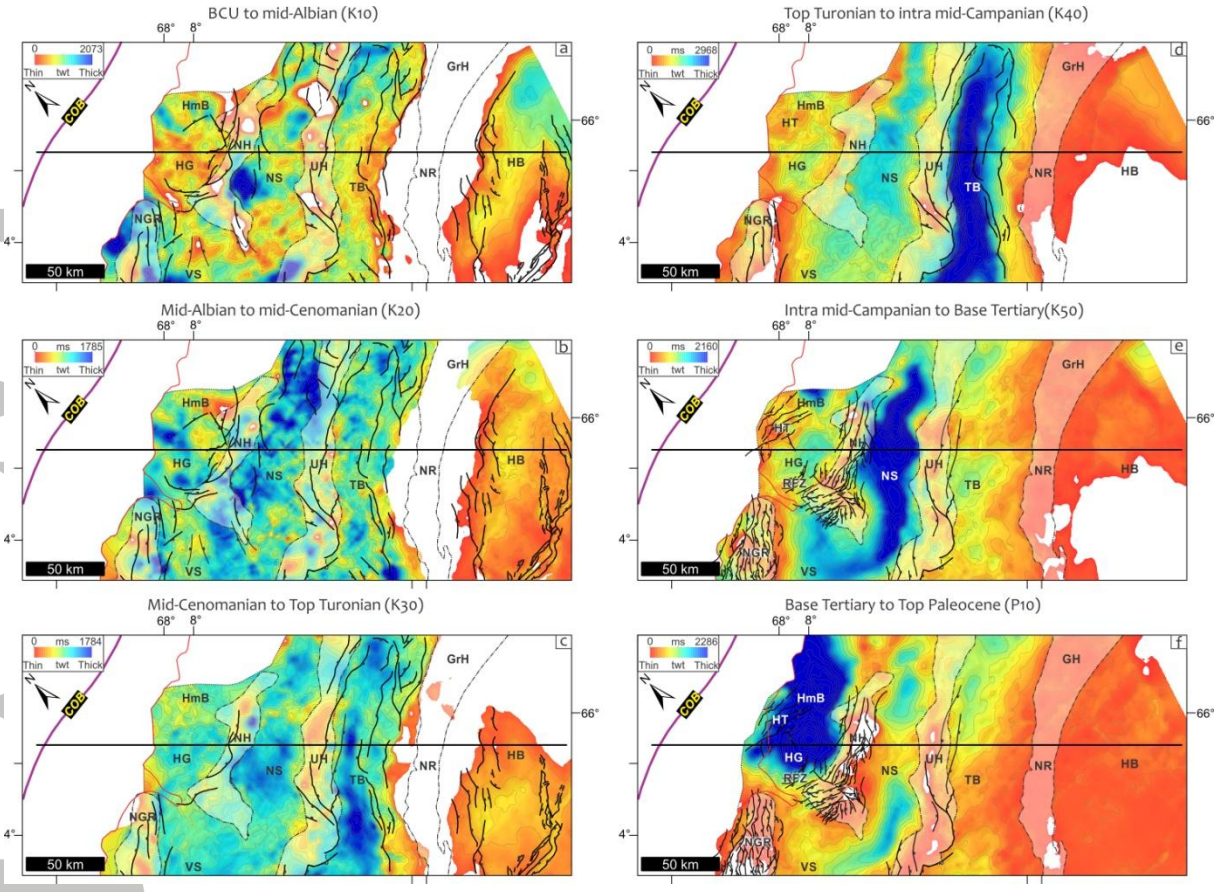

Figure 11. Isochore maps of seismic sequences K10 through P10 showing general distribution and migration of the basin depocentres in time and space. Present structural outline of the main structural highs are shown in transparent white. Extent of the maps is shown on the Figure 1a. GrH – Grønøy High, HB – Helgeland Basin, HG – Hel Graben, HmB – Hermod Basin, HT – Hel Terrace, NGR – North Gjallar Ridge, NH – Nyk High, NS – Någrind Syncline, RFZ – Rym Fault Zone, TB – Træna Basin, UH – Utgard High, VS – Vigrid Syncline.

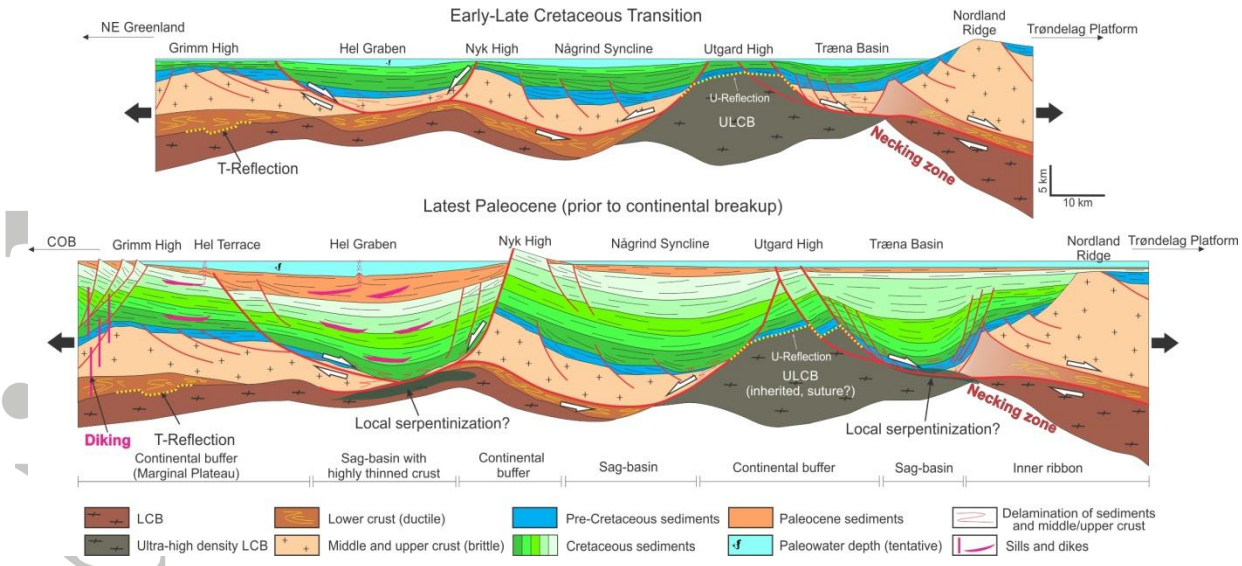

Figure 12. Cartoon illustrating Cretaceous-Paleocene evolution of the northern Vøring Margin.

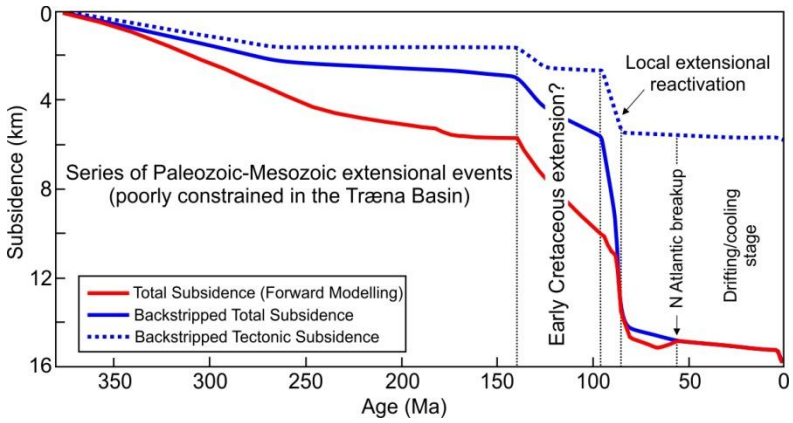

Figure 13. Total and tectonic subsidence curves calculated by different methods (forward modelling and backstripping) on the axial part of the Træna Basin. Extreme subsidence rates obtained for mid-Cenomanian-Santonian time are typical for strike-slip related basins, but also can be attributed to rift basins associated with steep-dipping faults. Subsidence curves were computed using the TecMod 2D software.

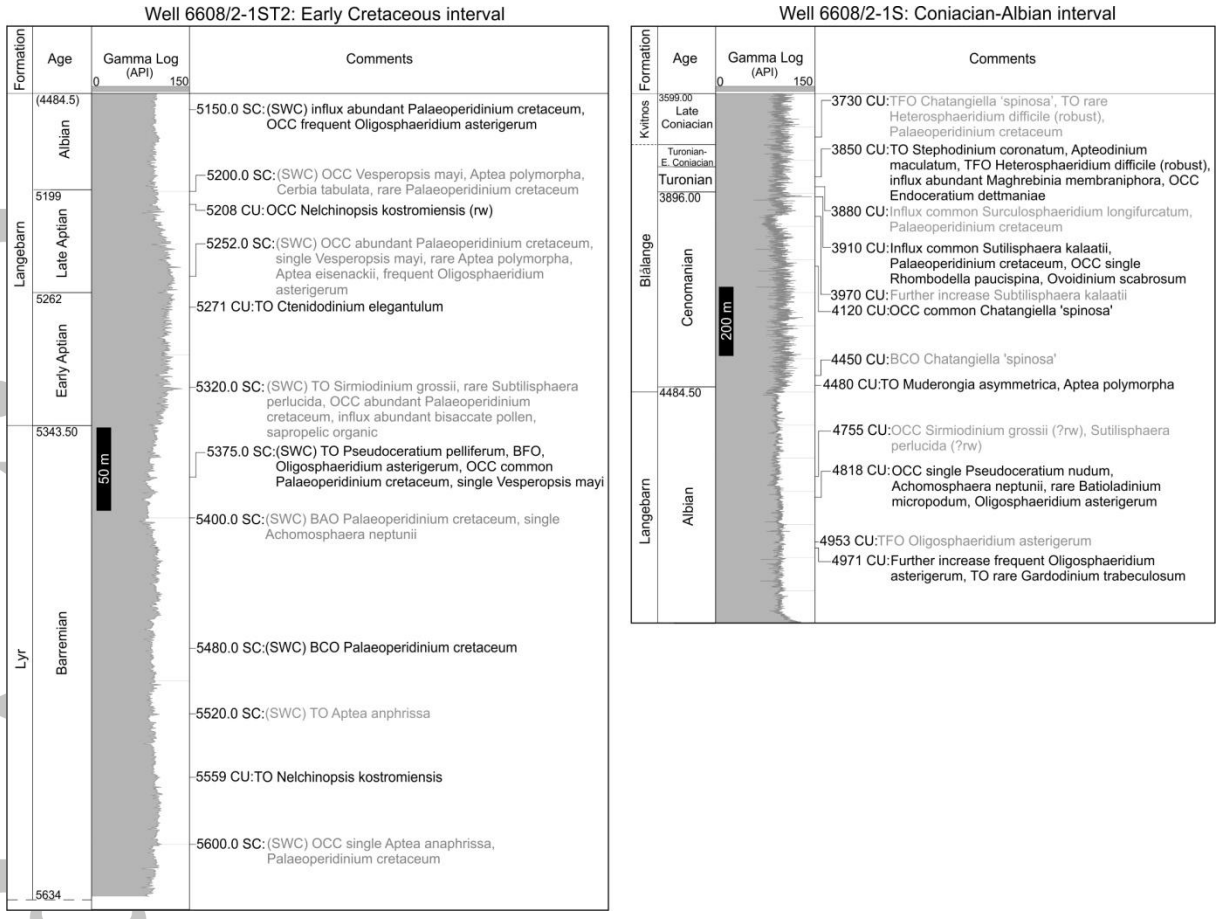

Figure A1. Well 6608/2-1S and ST2 bypass. Biostratigraphy summary chart of Barremian to Coniacian intervals. Formation names after NORLEX (Gradstein et al., 2010).

Table 1. Density and magnetic properties of the units modeled in the present study.

Layers	Density (kg.m^{-3})	Susceptibility (SI units)	Remanence (A/m)
Water	1450	0	0
Mid-Pliocene to Holocene	1800-1900	0	0
Mid-Miocene to Mid-Pliocene	2000	0	0
Eocene to Mid-Miocene	2050	0	0
Basalts/SDR	2550	0.01	-1 (Upper); +1 (Lower)
Paleocene	2225	0	0
Intra Mid-Campanian to Maastrichtian	2400	0	0
Lower Campanian to Intra Mid-Campanian	2400-2525 (deep sag)	0	0
Mid-Coniacian to Upper Santonian	2525-2575 (deep sag)	0	0
Mid-Cenomanian to Lower Coniacian	2525-2600 (deep sag)	0	0
Mid-Albian to Mid-Cenomanian	2550-2675 (deep sag)	0	0
Valanginian to Mid-Albian	2550-2700 (deep sag)	0	0
Pre-Cretaceous (und)	2650-2775 (deep sag)	0	0
Callovian to Berriasian	2500	0	0
Toarcian to Bathonian	2550	0	0
Hettangian to Pliensbachian	2559	0	0
Upper Triassic	2575	0	0
Mid-Triassic	2585	0	0
Mid-Permian to Lower Triassic	2600	0	0
Upper Devonian ?-Permian	2700	0	0
Upper crust (~Caledonian nappes)	2750	0.01	0
Middle Crust	2850	0.03	0
Lower Crust	2950	0.005	0
High density lower crust (LCB)	3100	0.005	0
Ultra-high density lower crust (ULCB)	3250	0.015	0
Mantle	3300(lower)-3250 (upper)	0	0